THE EFFECT OF AHOKO OIL SHALE ON THE ACTIVATION ENERGY OF THE CO-PYROLYSIS WITH POLYETHYLENE

BY

IRETIMIDE Eyitayo Ojuekaiye
MENG/SEET/2017/7297

**A THESIS SUBMITTED TO THE POSTGRADUATE SCHOOL
FEDERAL UNIVERSITY OF TECHNOLOGY, MINNA, NIGERIA
IN PARTIAL FULFILMENT OF THE REQUIREMENT FOR THE AWARD OF
THE DEGREE OF MASTER OF ENGINEERING
IN CHEMICAL ENGINEERING**

JANUARY, 2021

ABSTRACT

This study explored the effect of Ahoko oil shale on the activation energy in the co-pyrolysis with polyethylene. The study of optimization of oil yield from the co-pyrolysis of oil shale and Polyethylene was investigated at different temperature based on TGA and residence time of 90 mins. DESIGN EXPERT (Version 7.0.0, Stat Ease, Inc., USA) software was applied to investigate the oil recovery process to optimize the mixture compositions for maximum oil yield and to observe the blending behavior of the two samples in relation to oil yield. Analysis of variance (ANOVA) showed the model generated was significant with a p-value <0.0001, R^2 value of 0.9297, adjusted R^2 of 0.9329 and predicted R^2 of 0.9790. The optimum mixture composition for the oil yield was 50 % oil shale to 50 %. Dynamic pyrolysis and co-pyrolysis tests at different heating rates of 5, 10 and 15 ^oC/min were carried out using a thermogravimetric analyzer (TGA) to determine the kinetic parameters of the process. The obtained oils were characterized using Fourier transform infrared spectrometer (FT-IR) and Gas Chromatograph Mass Spectrometry (GCMS). The kinetics of pyrolysis and co-pyrolysis was determined via model-free iso-conversional methods, from the model, oil shale had an activation energy value of 45.19, 42.00, 44.55 and 46.32 kJ/mol with respect to Arrhenius, Flynn-wall-ozawa, Freidman and Coats-Redfen method respectively. The Polyethylene had an activation energy value of 153.14 154.64, 158.72, 155.41 kJ/mol in respect to Arrhenius, Flynn-wall-ozawa, Freidman and Coats-Redfen method respectively. The activation energy for the mixture was also calculated to be 52.95, 49.86, 51.04 and 52.33 kJ/mol with respect to Arrhenius, Flynn-wall-ozawa, Freidman and Coats-Redfen method respectively. Among the four models used for this work which used linear regression, the FWO method showed the best fit to the experimental TGA data for both oil shale, polyethylene and their mixture pyrolysis. The results showed that the activation energy of co-pyrolysis was evidently lower than that of polyethylene pyrolysis. This led to the conclusion that co-pyrolysis could be a potential method for obtaining shale oil due to the synergy between oil shale and polyethylene.

TABLE OF CONTENTS

LIST OF TABLES

LIST OF FIGURES

LIST OF PLATES

ABBREVIATION

XRD	-	X-Ray Diffraction
SEM	-	Scanning Electron Microscopy
FT-IR	-	Fourier Transform Infrared Spectra
GC-MS	-	Gas Chromatography - mass Spectrometry
RSM	-	Response Surface Methodology
TGA	-	Thermo-Gravimetric Analysis
DOE	-	Design of Experiment
CCD	-	Central Composite Design
HDPE	-	High Density Polyethylene
LDPE	-	Low Density Polyethylene
FWO	-	Flynn-Wall-Ozawa method
E_a	-	Activation Energy

CHAPTER ONE

1.0 INTRODUCTION

1.1 Background to the Study

Energy is essential to the economic and social development of life all over the world. The energy problem is a comprehensively discussed subject, and the number of concerns about the future of energy supply is increasing. Increase in oil prices, and environmental pollution course by fossil fuels, government policies and support for the construction of renewable production facilities in many countries, has increased the use of renewable energy sources. It is difficult for most renewable technologies to compete economically with fossil fuel over the planning stage. Renewable energy systems require electricity distribution and cogeneration (combined heat and power) with large capital cost. Therefore, these systems are usually founded on a small scale (Herzog, 2001).

In addition to renewable energy sources, there is also an interest in alternative energy sources due to the increasing energy requirement in recent years. Research for alternative energy has been intensified. Oil shale as a kind of alternative energy source has attracted more and more attention due to large reserves in Nigeria and the Africa in commercial potential (Taciuk, 2013). Oil shale is an organic-rich fine-grained sedimentary rock containing a great quantity of kerogen (10 to 65 wt% of the total mass) and mineral matrix (Martins *et al.*, 2010). The kerogen has high a hydrogen/carbon ratio, giving it the potential to be superior to heavy oil or coal as a source of liquid fuel. Oil shale is usually used as a source of fuel, solvent, chemical and other products after a thermal conversion process (Wang *et al*., 2012). Oil shale is the second largest fossil fuel source following the lignite reserves. The calorific value of oil shale varies between 500 and 4500 kcal/kg. Therefore, a detailed study must be made on the possible use for each reserve (Altun *et*

al., 2009). Owing to its importance in energy utilization, effective and economic

utilization of oil shale is under intensive study (Kılıç *et al.,* 2014). Among many conversion processes, pyrolysis is an efficient energy conversion technology. Pyrolysis of oil shale leads to the production of gases, liquid (water and tar) and char. Recently, co-pyrolysis has become an attractive method for a variety of economic reasons: in-place evaluation of fossil fuels, reduction in the volume of waste and recovery of chemicals (Espina *et al.,* 2015). Research on the copyrolysis process is generally focused on the synergistic effect. All improvements in pyrolysis oil quality and quantity during copyrolysis occur through synergistic effects. This effect depends on the type of feedstock, pyrolysis duration, temperature, heating rate, removal or equilibrium of volatiles formed, and addition of catalysts (Abnisa *et al.,* 2015).

The type of feedstock is important among these factors; thus, synergistic effects on copyrolysis can be changed based on feedstock. The co-pyrolysis method can be an environmentally friendly way for the conversion of oil shale and plastic waste into valuable products. The use of plastics in our daily life has increased rapidly during the last few decades. The amount of waste plastics discarded each year is constantly increasing and is causing serious environmental problems. Many of the plastic waste are evaluated by inappropriate environmental regulations for disposal methods such as incineration or landfill. Therefore, plastic recycling has become a necessity. Due to the increased environmental awareness and depletion of natural oil deposits, the conversion of waste plastics into liquid hydrocarbons has been considered a promising recycling method. Conversion of plastic waste to energy and chemical raw materials is provided by pyrolysis. However, it has been suggested that the addition of plastic into the coal during pyrolysis process may result in an increased coal conversion and liquid yield when compared to that obtained when coal alone is pyrolyzed (Zahid *et al*., 2016). Plastic waste materials could act as an inexpensive hydrogen source aiding the dissolution of coal

during the thermal co-processing with mining materials with less hydrogen content such as oil shale, coal or biomass (Bozkurt *et al*., 2017). Product yield and its composition in co-pyrolysis of coals with plastic materials depend on the type of plastic. Having a high hydrogen-to-carbon ratios and convenient molecular chain structure, waste commodity plastics such as low and high density, polyethylene, polyethylene terephthalate (PET), polystyrene (PS), and polyvinyl chloride (PVC) are suitable for liquid production (Salepcioglu *et al*., 2008). Among these, low and high density, polyethylene is such a polymer, used for various purposes. The use of polyethylene composes massive waste which cannot be recycled completely.

Furthermore, the recycling process consumes huge amounts of energy and also produces low quality polymer. Co-pyrolysis of plastic waste materials with oil shale has been studied by a few authors in recent years and these studies indicated a synergistic effect for co-pyrolysis of oil shale and plastic waste mixtures in the form of enhanced liquid yields. Bozkurt *et al*. (2017) investigated the pyrolysis of Moroccan oil shale and plastic mixtures by thermogravimetric analysis. In all mixtures containing Moroccan oil shale and high-density polyethylene (HDPE), low density polyethylene (LDPE) and polypropylene (PP), the maximum degradation temperatures of each component were higher than those of the individual components (Bozkurt *et al*., 2017). The experimental results indicated a significant synergistic effect leading to an increase in thermal stability during co-pyrolysis. On the other hand, in co-pyrolysis of Tarfaya oil shale with plastics, experiments were performed in an autoclave reactor and the effects of the heating rate and pyrolysis temperature on product yields were investigated (Aboulkas *et al*., 2012). The results indicated that co-pyrolysis process leads to the higher oil yields compared with individual pyrolysis of oil shale. Recently, in another co-pyrolysis study made by the same group, it investigated a detailed characterization of the oil obtained by

copyrolysis of Tarfaya oil shale and high density, polyethylene (HDPE) and by pyrolysis of oil shale and HDPE individually (Aboulkas *et al*., 2012). Conversion into volatile hydrocarbons was found lower with increasing LDPE ratio in oil shale-LDPE mixture while C_{16} hydrocarbons and the amount of coke deposit were higher in the presence of LDPE. The objective of the present study is to determine the synergetic effect in co-pyrolysis of oil shale and low density, polyethylene (LDPE) with the aim of determining the activation energy of the process. For this reason, this work seeks to examine the suggestion of fixed bed co-pyrolysis of Ahoko oil shale with polyethylene at the ratio based on design expert.

1.2 Statement of the Research Problem

Energy is essential to the economic and social development of life all over the world. The energy problem is a comprehensively discussed subject, and the number of concerns about the future of energy supply is increasing. The use of plastics in our daily life has increased rapidly during the last few decades. The amount of waste plastics discarded each year is constantly increasing and it causes serious environmental problems. Many of the plastic waste are evaluated by inappropriate environmental regulations for disposal methods such as incineration or landfill and therefore, the need to convert this consistent waste into a useful product.

1.3 Aim and Objectives of the Study

The aim of this research work is examine the effect of co-pyrolysis of Ahoko oil shale and Polyethylene on the oil yield. The aim will be achieved through the following objectives.

i Characterization of the oil shale and Polyethylene

ii To determine the effect of polyethylene on co-pyrolysis of the oil shale.

iii To study kinetics of the process and determine the improvement in the activation energy.

iv Characterization of the product of the pyrolysis

1.4 Scope of the Study

The research work is limited to the study of the effect of co-pyrolysis of Ahoko oil shale and Polyethylene on its activation energy and oil yield.

1.5 Justification of the Study

Oil shale and plastics are available in Nigeria and this could be used to produce crude oil product which in turn is used to drive the economy as energy source. Plastics which are used in daily life result to environmental problems if not properly disposed off. However, it could be used to decrease the energy requirement for production of oil from oil shale. Also, it is necessary to know the peculiar behavior of Ahoko oil shale when it is being copyrolised with polyethylene and its effect on the yield of its resultant oil.

CHAPTER TWO

2.0 LITERATURE REVIEW

2.1 Oil Shale

Oil shale is a sedimentary rock with characteristic low porosity and less permeability, the soluble part of oil shale is called bitumen while the insoluble part is called kerogen (Zhang *et al*., 2019). Oil shale is a natural rich fine-grained sedimentary rock containing kerogen (from which fluid hydrocarbons can be delivered, called shale oil (not to be mistaken for tight oil raw petroleum happening normally in shale). Shale oil can replace the traditional raw petroleum; in any case, removing shale oil from oil shale is more expensive than the creation of regular unrefined petroleum both monetarily and as far as its ecological impact. Oil shale is a natural rich fine-grained sedimentary shale containing kerogen (a strong blend of natural synthetic mixes) from which fluid hydrocarbons can be delivered, called shale oil (not to be mistaken for tight oil raw petroleum happening normally in shale oil (Ma *et al*., 2020). Shale oil is an unconventional oil produced from oil shale rock fragments by pyrolysis, hydrogenation, or thermal dissolution. These processes convert the organic matter within the rock (kerogen) into synthetic oil and gas. The resulting oil can be used immediately as a fuel or upgraded to meet refinery feedstock specification by adding hydrogen and remove impurity such as sulfur and nitrogen.

The refined products can be used for the same purposes as those derived from crude oil. The term "shale oil" is also used for crude oil produced from shales of other very low permeability formations. However, to reduce the risk of confusion of shale oil produced from oil shale with crude oil in oil-bearing shales, the term "tight oil" is preferred for the latter (Demirbas, 2016). The International Energy Agency recommends to use the term "light tight oil" and World Energy Resources 2013 report by the World Energy Council uses the term "tight oil" for crude oil in oil-bearing shales.

Oil shale was one of the first sources of mineral oil used by humans. In the 10th century, the Arabic physician Masawaih al-Mardini (Mesue the Younger) first described a method of extracting oil from "some kind of bituminous shale" (Forbes, 1970). It was also reported to have been used in Switzerland and Austria in the early 14th century. In 1596, the personal physician of Frederick I, Duke of Württemberg wrote of its healing properties (Salepcioglu *et al*., 2008). Shale oil was used to light the streets of Modena, Italy at the turn of the 18th century. The British Crown granted a patent in 1694 to three persons who had "found a way to extract and make great quantities of pitch, tarr and oyle out of a sort of stone (Boak and Kleinberg, 2016). Later sold as Betton's British Oil, the distilled product was said to have been "tried by diverse persons in Aches and Pains with much benefit (Forbes, 1970). Modern shale oil extraction industries were established in France during the 1830s and in Scotland during the 1840s. The oil was used as fuel, as a lubricant and lamp oil; the Industrial Revolution had created additional demand for lighting. It served as a substitute for the increasingly scarce and expensive whale oil (Dyni and John 2010).

2.2 Methods of Production of Oil Shale Process

Shale oil is extracted by pyrolysis, hydrogenation, or thermal dissolution of oil shale (Luik *et al*., 2009). The pyrolysis of the rock is performed in a retort, situated either above ground or within the rock formation itself, most oil shale industries perform the shale oil extraction process after the rock is mined, crushed and transported to a retorting facility, although several experimental technologies perform the process in place (*in-situ*).The product is then blended to meet up pipe line standard for crude oil.

The production of shale oil is divided into two: in-situ (subsurface) and exsitu (surface).

In 1684, Great Britain performed the first extraction. This process spread wide in the 19th century. In-situ method is recognized to be an effective way of obtaining largescale

production from oil shale. The established heating technique include Shell's *insitu* Conversion Process (ICP) technology (Brandt, 2008; Kar and Hascakir, 2017), gas (overheated air, CO_2, or hydrocarbon) injection to heat oil-shale beds (Bauman and Deo, 2012; Zhao *et al*., 2020), microwave and other radiation heat technologies (AlGharabli *et al*., 2015; Mokhlisse *et al*., 2000). Many of these technologies are either terminated or still in the stage of demonstration due to some technical defects. Therefore, it is critical and urgent to develop an economically feasible *in-situ* retorting technology for oil and gas extraction from oil shale. The temperature at which the kerogen decomposes into usable hydrocarbons varies with the time-scale of the process; in the above-ground retorting process decomposition begins at 300 °C, but proceeds more rapidly and completely at higher temperatures. Decomposition takes place most quickly at a temperature between 480 and 520 °C (Luik *et al*., 2009).

Hydrogenation and thermal dissolution (reactive fluid processes) extract the oil using hydrogen donors, solvents, or a combination of these. Thermal dissolution involves the application of solvents at elevated temperatures and pressures, increasing oil output by cracking the dissolved organic matter. Different methods produce shale oil with different properties, (Koel *et al*., 2001; Gorlov *et al*., 2007). A critical measure of the viability of extraction of shale oil lies in the ratio of the energy produced by the oil shale to the energy used in its mining and processing, a ratio known as "Energy Returned on Energy Invested".

2.3 Property of Oil Shale

The properties of raw shale oil vary depending on the composition of the parent oil shale and the extraction technology used (McKetta, 1994). Like conventional oil, shale oil is a complex mixture of hydrocarbons, and it is characterized using bulk properties of the oil.

Shale oil usually contains large quantities of olefinic and aromatic hydrocarbons. Shale oil can also contain significant quantities of heteroatoms. A typical shale oil composition includes 0.5–1 % of oxygen, 1.5–2 % of nitrogen and 0.15–1 % of sulfur, and some deposits contain more heteroatoms. Mineral particles and metals are often present as well, (Speight, 2008). Generally, the oil is less fluid than crude oil, becoming pourable at temperatures between 24 and 27 °C, while conventional crude oil is pourable at temperatures between 60 to 30 °C; this property affects shale oil's ability to be transported in existing pipelines (Wauquier *et al*., 1995).

Shale oil contains polycyclic, aromatic hydrocarbons which are carcinogenic. It has been described that raw shale oil has a mild carcinogenic potential which is comparable to some intermediate refinery products, while upgraded shale oil has lower carcinogenic potential as most of the polycyclic aromatics are believed to broken down by hydrogenation.

2.4 Uses of Shale Oil

Before World War II, most shale oil was upgraded for use as transport fuels. Afterwards, it was used as a raw material for chemical intermediates, pure chemicals and industrial resins, and as a railroad wood preservative. As of 2008, it is primarily used as a heating oil and marine fuel, and to a lesser extent in the production of various chemicals (Speight, 2008). Shale oil's concentration of high-boiling point compounds is suited for the production of middle distillates such as kerosene, jet fuel and diesel fuel (Speight, 2008).

2.5 Ahoko Oil shale

Ahoko oil shale is predominately found in part of the Bida basin. It comprises hydro carbon seepages in the basins around Pategi/Muregi on the River Niger in Niger State and around Ahoko near Lokoja in Kogi State, Ahoko is 49 km from Lokoja on the Lokoja,

Abuja express way (Adeoye *et al*., 2020). The argillaceous units of the Patti formation are well exposed. The approximately 26 m thick section level consists predominantly of shales and siltstones which are rhythmically interbedded with concrete to massive bioturbated ironstone at the basal part of the section is a predominant shale bed with average thickness of 0.5 m. The shales are dark to light grey (Adeoye *et al*., 2020).

The study areas are located at Ahoko 49 km from Lokoja where the deepest part of the Patti Formation is exposed along Lokoja-Abuja expressway. The studied outcrops are road cut sections with coordinates of longitude N 006005’27.9‖, latitude E 008018’6.1‖ with an elevation of 88m and the Ahoko Quarry with longitude N 006051’26.7‖, latitude E 008078’15.0‖ and an elevation of 94m respectively. The generation of oil shale from Ahoko rock was investigated using Total Organic Carbon and Rock-Eval pyrolysis analyses on the rock. It was obtained that the rock is organically rich and TOC values up to 2.49 % indicating enormous deposit of oil whereby Plate I: shows the photograph of the sequence of deposit of the heterolithic beds at Ahoko.

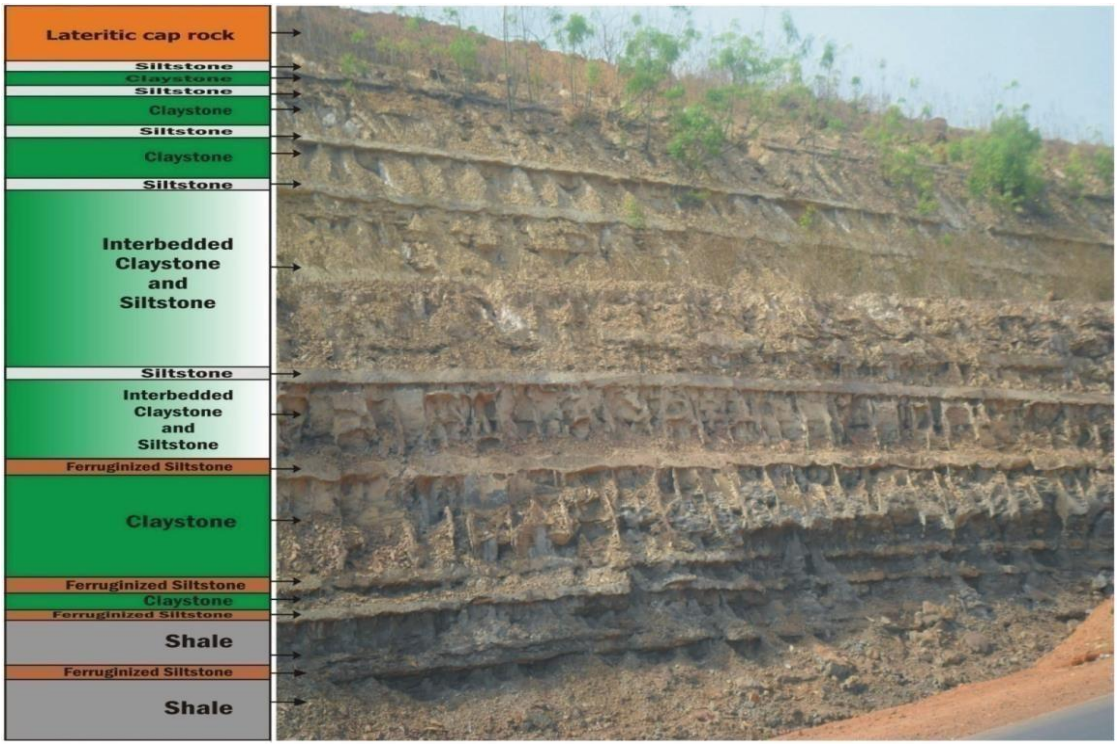

Plate I: Photograph showing the sequence of deposition of the heterolithic beds at Ahoko

2.6 Oil Shale Reserves

United States of America (USA) has the largest oil shale reserve located in the Green river formation (Hoe, 2014).). It had been seen that oil shale is widely distributed in the world, hence a technology to improve it recovery was been developed (Dell *et al*., 2014). Conventional oil reserves can be substituted by the vast resources of petroleum generating source rock known as oil shale. There are significant resources of oil shale in Nigeria and the world at large, which if exploited in an environmentally safe manner, would provide secure source of transportation fuels. An oil shale reserve refers to oil shale resources that are economically recoverable under current economic conditions and technological abilities (Youngquist, 1998). Oil shale deposits range from small presently economically unrecoverable to large potentially recoverable resources
(Youngquist, 1998). Defining oil shale reserves is difficult, as the chemical composition of different oil shales, as well as their kerogen content and extraction technologies, vary significantly.

The economic feasibility of oil shale extraction is highly dependent on the price of conventional oil; if the price of crude oil per barrel is less than the production price per barrel of oil shale, it is uneconomic (Youngquist, 1998). As source rocks for most conventional oil reservoirs, oil shale deposits are found in all world oil provinces, although most of them are too deep to be exploited economically. There are more than 600 known oil shale deposits around the world (Youngquist, 1998). Although resources of oil shale occur in many countries, only 33 countries possess known deposits of possible economic value (Youngquist, 1998). Many deposits need more exploration to determine their potential as reserves. Well-explored deposits, which could ultimately be classified as reserves, include the Green River deposits in the western United States, the

Tertiary deposits in Queensland, Australia, deposits in Sweden and Estonia, the ElLajjun deposit in Jordan, and deposits in France, Germany, Brazil, China, and Russia. Therefore, Plate II: shows location of oil shale in the world in order of decreasing reserve and it is expected that these deposits would yield at least 40 liters (0.25 bbl) of shale oil per metric ton of shale, using the Fischer Assay (Youngquist, 1998).

Plate II: Location of oil shale in the world in order of decreasing reserve

2.7 Environmental Issue Associated with Shale Oil Production

Oil shale imposes a very severe effect on the environment because it contains significant amount of nitrogen and sulphur which can cause acid rain upon reaction (Juraj *et al*., 2017). The extraction and processing of oil shale cause environmental issue such as land use, waste management, water and air pollution (Juraj *et al*., 2017). The surface mining of oil shale requires large area of land (Juraj *et al*., 2017). The mining of oil shale reduces the original ecosystem diversity that should be able to support variety of animal and plant

(Juraj *et al*., 2017). The disposal of waste from mining process which include spent oil shale and semi-coke need large area of land (Juraj *et al*., 2017). According to the United States, production of one barrel of shale oil will produce 1.5 tonnes of semi-coke. The waste of oil shale consists of several pollutants which include sulphates, polycyclic aromatic hydrocarbons and heavy metals which can affect the groundwater.

2.8 Basic Concept of Waste Plastic

In today's modern world, plastic provide a fundamental contribution to all activities such as agriculture, automobile industry, electricity and electronic, building materials, packing. Increased production of plastic leads to generation of enormous amounts of waste. Most of these plastics are still disposed of by landfill. Incineration of plastics is not the way to increase their value and the consequent energy recovery is not considered fully acceptable by current policies. Upgrading of plastic waste is a necessity both for environmental protection and for sustainable development. From these points of view, addition of plastic waste to feedstock of natural organic materials thermal processes can be a perspective for their conversion into valuable products (Tiikma *et al*., 2004). Much attention has been directed towards the use of plastic waste and its combination with oil shale. Co-processing techniques have received much attention in recent years because they should be considered as a beneficial process of recovering valuable hydrocarbons and recycling the waste materials with advantageous environmental and economic effects.

2.8.1 Polyethylene

Polyethylene is a kind of saturated polyester of terephthalic acid and ethylene glycol with high properties, high stiffness and safety. Due to its resistance to strong acid, oxidizing agents and microorganisms, it has been widely used as bottle materials, fibres, films, sheets, households and carpet (Levchik and Weil, 2004; Datta and Kopczyn´ ska, 2016).

The worldwide consumption and demand of PET reached about 60 million tons and grew at about 4.5 % each year.

2.8.2 Properties of polyethylene

There are many properties of polyethylene which are; mechanical, chemical and Electrical properties. The mechanical properties are very dependent on the molar weight and on the degree of branching of the polymer. As with other polymers these properties are also dependent on the rate of testing, the temperature of test, the method of specimen preparation, the size and shape of the specimen, and, to only a small degree with polyethylene (PE), the conditioning of samples before testing. The chemical Properties are properties which show the chemical resistance of PE is, to a large measure that expected of an alkane. It is not chemically attacked by monoxidizing acids, alkalis, and many aqueous solutions. Nitric acid oxidizes the polymer, leading to a rise in power factor and to deterioration in mechanical properties. As with the simple alkanes, halogens combine with the hydrocarbon by means of substitution mechanisms. Oxidation of PE which leads to structural changes can occur to a measurable extent at temperatures as low as 50 ^{o}C under the influence of ultraviolet light the reaction can occur at room temperature. The oxidation reactions can occur during processing and may initially cause a reduction in melt viscosity.

Further oxidation can cause discoloration and streaking, and in the case of polymers rolled for 1.2 h on a two-roll mill at about 150 ^{o}C, the product becomes ropey and incapable of flow. It is rare that such drastic operating conditions occur but it is found that at a much earlier stage in the oxidation of the polymer there is a serious deterioration in power factor, and for electrical insulation applications in particular it is necessary to incorporate antioxidants. It is to be expected that the less branched high density polyethylene (HDPE),

because of the smaller number of tertiary carbon atoms, would be more resistant to oxidation. That this is not always the case has been attributed to residual metallic impurities, since purer samples of high-density polymers are somewhat superior to the low density materials while Electrical properties most time refer to as insulating properties of PE compare favorably with those of any other dielectric material. As it is a nonpolar material, properties such as power factor and dielectric constant are almost independent of temperature and frequency. Dielectric constant is linearly dependent on density and a reduction of density on heating leads to a small reduction in dielectric constant. Oxidation of PE with the formation of carbonyl groups can lead to a serious increase in power factor. Antioxidants are incorporated into compounds for electrical applications in order to reduce the effect.

2.9 Kerogen

Oil shale is a fine-grained sedimentary rock which consists of an inorganic mineral matrix containing a cross-linked macromolecular organic matter called kerogen (Datangel and Goldfarb, 2011). The chemical formula of kerogen is $C_{200}H_{300}SN_5O_{11}$ with an average molecular weight of 3000 (McCarthy *et al*., 2011).

2.9.1 Pyrolysis of kerogen

The kerogen in oil shale, in its natural state, is completely solid and is not recoverable as natural oil or gas in the reservoir. Only after retorting (pyrolysis) (Kang *et al*., 2011), the kerogen in the oil shale could be converted into liquid shale oil and gas (Tao *et al*., 2012). The property and composition depends on it location. It is a heterogeneous compound. The breaking down of kerogen into by product when subjected to retorting or heat is termed pyrolysis (Juraj *et al*., 2017). The pyrolysis of oil shale is analogous to the method of producing conventional oil. Shale oil and gas production is referred to as

unconventional because it is treated artificially at a faster rate. Upon application of heat, volatile materials are produced (McCarthy *et al*., 2011). This volatile material ranges from light organic and inorganic gas to heavy liquid. The condensation of this product gives rise to shale oil and shale gas. There are series of reaction that occurs during the pyrolysis of oil shale. It can be summarized into two: Primary and secondary pyrolysis (McCarthy *et al*., 2011). The shale gas produce is very light hydrocarbon and inorganic gases, carbon dioxide and hydrogen while the shale oil is a mixture of heavy and light oil when the vapor and liquid are at equilibrium (McCarthy *et al*., 2011). The water generated in this process are free water and bound water that was produced from organic and decomposition of minerals (McCarthy *et al*., (2011)

$$\text{Organic Matter} \longrightarrow \text{Oil} + \text{Char} + \text{Gas} + H_2O \qquad (2.1)$$

The reaction of Equation 2.1, shows is the simplest mechanism for the representation of oil shale pyrolysis. Liquid and gas produced from the pyrolysis of the Kerogen contains Coke, gas and oil. The oil produced contains liquid and gas which includes coke, gas and oil. The char produce contains gas and carbonaceous residue (McCarthy *et al*., 2011).

2.9.2 Classes of oil shale pyrolysis technology

The oil shale pyrolysis technology can be classified into two main categories, which are aboveground retorting technology and underground retorting technology. Aboveground retorting technology deals with the use of large-scale installed systems on the ground to produce a high-temperature anaerobic environment (Wang *et al*., 2014). In this process, the mined oil shale is crushed to a specific size, transferred to the aboveground pyrolytic system, and then returned to produce shale oil and gases (Bai *et al*., 2015). There are problems associated to this technology these include; slag occupation, inefficiencies and environmental unfriendliness (Selberg *et al*., 2011; Raukas and Punning, 2009) while underground retorting technology avoids the retorting at the surface. This technology is

economically ineffective and it's difficult to operate (Kang *et al*., 2020). This technique is divided into (i) In-situ artificial crushing and retorting and (ii) real underground insitu retorting.

2.9.3 Pyrolysis mechanism of oil shale

The organic matter of oil shale is composed of aliphatics, aromatics, and some heteroatomic functional group, which causes pyrolysis. There are mainly three kinds of chemical reactions in the pyrolysis process: reaction of aliphatics, aromatics, and heteroatomic functional group (Wang *et al*., 2014). The pyrolysis reactions of aliphatic hydrocarbons are the carbon– carbon and carbon–hydrogen bond's rupture of n-alkanes, isoparaffin, cycloalkane, olefin, which are endothermic, the reaction of aromatics contains dehydrogenation, condensation, and carbonation reaction of alkylate, which are exothermic, while The reaction of heteroatomic functional group contains decarboxylation, dehydroxylation, deamination, and desulphation were express in Equation 2.2, 2.3, 2.4 and 2.5 respectively. This reaction determines the content of NH_3, CO_2, and element of S, N, and has little influence on the quality of shale oil.

Decarboxylation: $RCOOH \longrightarrow RH + CO_2$ 2.2

Dehydroxylation: $RCH_2CH_2OH \longrightarrow RCH = CH_2 + H_2O$ 2.3

Deamination:

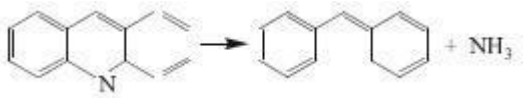

2.4

Desulphation:

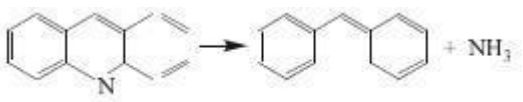

2.5

2.9.4 Pyrolysis of polyethylene

Fundamentally, different types of plastics have different compositions that normally reported in terms of their proximate analysis. Proximate analysis can be defined as a technique to measure the chemical properties of the plastic compound based on four particular elements which are moisture content, fixed carbon, volatile matter and ash content. Volatile matter and ash content are the major factors that influence the liquid oil yield in pyrolysis process. High volatile matter favored the liquid oil production while high ash content decreased the amount of liquid oil, consequently increased the gaseous yield and char formation.

Vijayakumar and Sebastian (2018) have investigated the LDPE pyrolysis in fixed-bed reactor at 500 ^{o}C with heating rate of 10 ^{o}C/min. The experiment was done for duration of 20 min and nitrogen was used as fluidizing gas. It was observed that high liquid yield of 95 wt % was obtained with low gas yield and negligible char. High liquid oil yield of 93.1 wt % has also been obtained by Marcilla *et al*. (2010) when the experiment was carried out in a batch reactor at 550 ^{o}C, but this time with lower heating rate of 5 ^{o}C/min. There are also some researchers who studied the LDPE pyrolysis at lower operating temperature less than 500 ^{o}C. From the research conducted by Vijayakumar and Sebastian (2018) using batch reactor at 430 ^{o}C, the liquid yield obtained was around 75.6 wt %, have obtained a closer yield with which was 74.7 wt % when using the same type of reactor at 450 ^{o}C. However, the liquid oil yield could be increased when pressure was applied in the reactor during the process, even though at lower temperature.

2.9.5 Co-pyrolysis of polyethylene and oil shale

Salepcioglu *et al*. (2008) showed an increase in gas yield for co-pyrolysed oil shale and LDPE, as the temperature of pyrolysis was increased which was attributed to gas phase cracking reactions to yield increased hydrocarbons. Additionally, it can be seen that gaseous n-paraffins and 1-olefins constitute the highest portion of the pyrolysis products. As temperature increases, the amounts of gaseous products increase which results as an increase in aliphatic hydrocarbon recovery. Co-pyrolysis of heavy shale oil with polyethylene waste in an autoclave at various temperatures and times has been studied, and it was found that co-pyrolysis improves the quality of oil and gives possibility to convert the wastes into liquid fuels. Temperature-programmed copyrolysis of two Turkish oil shales (shale oil content by Fisher assay 31.8 and 6.4 wt. %) with low-density PE (LDPE) was investigated. The kerogen type was found not to have a great effect on hydrocarbon distribution, but the experimental results indicated that the conversion of LDPE can be increased by catalytic effect of mineral materials. Spent shale (the residue after retorting Israeli oil shale at 500 to 550 °C) was used as a solid fuel constituent in mixture with waste rubber and plastics. The spent shale played the role of a heat-transfer medium, and of a mechanical carrier of the processed polymers.

Aboulkas *et al*. (2008) performed thermal degradation processes for a series of mixtures of oil shale/plastic using thermogravimetric analysis (TGA) at four heating rates of 2, 10, 20 and 50 K min^{-1} from ambient tem-perature to 1273 K. High density polyethylene (HDPE), low density polyethylene (LDPE) and polypropylene (PP) were selected as plastic samples. The overlapping degradation temperature of oil shale and plastic in TG/DTG curves of the mixture may provide an opportunity for free radicals from oil shale pyrolysis to participate in reactions of plastic decomposition. Gersten *et al*. (2000) investigated the thermal decomposition behaviour of polypropylene, oil shale and 1:3

mixtures of the two in a TG/DTG reaction system in an argon atmosphere. Experiments were conducted at three heating rates in the temperature range of 300 to 1173 K. The results indicated that the characteristics of the process depend on the heating rate, and the polypropylene acts as a catalyst in the degradation of oil shale in the mixture.

Degirmenci and Durusoy (2005) used the thermogravimetry analysis to obtain kinetics of the pyrolysis of oil shale, polystyrene and their mixtures. Experiments were carried out at non-isothermal decomposition conditions under argon atmosphere from 298 to 1173 K at heating rate values of 10 and 60 K min^{-1}. An increase was observed in the total conversion values of the blends with the increase in the blending ratio of polystyrene to oil shale. When a blend in any proportion of polystyrene to oil shale was degraded, an increase in maximum decomposition rate and a decrease in the temperature of maximum decomposition rate with the increase in polystyrene content of the sample were observed. The main conclusion is that the polystyrene accelerates the decomposition of the organic matter in the oil shale.

Thermogravimetric analysis and kinetics of coal/plastic blends during co-pyrolysis in nitrogen atmosphere were investigated by Cai *et al*. (2008). The results indicated that plastic was decomposed in the temperature range 711 to 794 K, while the thermal degradation temperature of coal was 444 to 983 K. The overlapping degradation temperature interval between coal and plastic was favourable for hydrogen transfer from plastic to coal. The difference of weight loss between experimental and theoretical ones, calculated as an algebraic sum of those from each separated component, was 2.0 to 2.7 % at 823 to 923 K. These experimental results indicated a synergistic effect during plastic and coal co-pyrolysis at the high temperature region. The overlapping degradation temperature of coal and plastic in TG/DTG curves of the mixture may provide an opportunity for free radicals from coal pyrolysis to participate in reactions of plastic

decomposition. Vivero *et al*. (2012) studied the thermal decomposition of blends of coal and plastic such as high density polyethylene and polypropylene using the thermogravimetric method. It was shown that plastic wastes have a strong influence on the thermoplastic properties of coal as well as the structure and thermal behaviour of the semicokes.

2.10 Kinetics of Thermal Decomposition

Oil shale sample from Mudanjiang, China was carried out were the kinetics of thermal decomposition was also determine (Liu *et al*., 2020). The samples was ground and sieved to corresponding sizes for different uses. Pyrolysis experiments were carried out using a TA SDT-Q600 analyzer, with the heating rate of 20 ^{0}C/min to a final temperature of 900 ^{0}C. About 20 mg of oil shale was put into the sample crucible. About 80 mL/min of high purity nitrogen as a carrier gas was made to flow through the reactor during the experiment. It was noted that the weight loss (TG) curves of oil shale in relation to the heating rate to the final temperature of 900 ^{o}C. It can be seen that there are three stages in the TG figures of pyrolysis process of oil shale.

The first stage is called the low-temperature weight loss step (stage 1), and it occurs in the range of room temperature to 200 ^{o}C. It is mainly caused by the precipitation of internal water and the layer water of clay mineral. It accounts for 5 % of the total weight loss. The second stage is called the decomposition of OM (stage 2), and it occurs in the range of 200 to 600 ^{o}C. During stage 2, weight loss occurs that has been attributed to the decomposition of hydrocarbons, with the escaping of oil and gas steam. This section accounts for about 70 % of the total weight loss. The last stage is called pyrolysis of carbonate (stage 3), and it occurs in the range of 600 to 900 ^{o}C. During stage 3, the weight loss is mainly caused by the decomposition of clay and carbonate minerals. The rate of

weight loss is distinctly lower than that of the second stage (Quan *et al*., 2016; Wang *et al*., 2012).

The RockEval pyrolysis method has been widely used for oil and gas exploration in sedimentary basins all over the world. This technique uses temperature programmed heating of a small amount of oil shale in an inert atmosphere (helium or nitrogen) in order to determine the quantity of free hydrocarbons present in the sample and of those that can be potentially released after pyrolysis.

2.10.1 Kinetic Parameter estimation from TGA data

Thermogravimetric Analysis or TGA is a common technique to determine global kinetic parameters for complex reactions parameters Freeman and Carroll, (1958); Shao *et al*., 2008). TGA analysis has been used in many industries ranging from coal char oxidation to analysis of sewage sludge pyrolysis (Selberg *et al*., 2011). These global kinetic parameters that is, the activation energy and pre-exponential factor used in the Arrhenius equation are useful from a modeling and engineering standpoint to describe reaction behavior.

Thermogravimetric involves the measurement of the mass of the sample while heating the sample. As the sample heats up it reacts and mass is released in the form of a vapor or gas. There are two common TGA systems employed: open systems and closed systems. An open system is so named because the sample is exposed to a sweep substance that constantly replaces the medium around the sample and sweeps the products away. This sweep substance is often a well-controlled gas atmosphere. The closed system consists of a sample isolated in a reaction cell, and reaction products persist around the sample. In a closed system some of the reaction products may react with and be reincorporated into the sample. A majority of systems utilize a controlled atmosphere of gases, but one

specialized form of a closed TGA utilizes water as the medium and a magnetic balance (Mochidzuki *et al*., 2003).

Generally mass loss measurements are made at either isothermal conditions or at a constant heating rate. One of the two aforementioned general methods, isothermal, is performed by heating the sample as quickly as possible to the reaction temperature and holding the sample at that temperature while recording the mass versus time. This has been a technique utilized by many researchers (Williams and Ahmad, 2000). An isothermal analysis is often carried out by plotting the rate constant from multiple experiments of various temperatures against the inverse of temperature on a log plot. The activation energy, E, is determined from the slope and the kinetic frequency factor is determined from the intercept. Non-isothermal studies involve heating a sample in an apparatus, often linearly with time at constant heating rate, and measuring the weight with respect to time or temperature. Time and temperature are usually related through some algebraic expression shown in Equation 2.6.

$$T = H \times t + T_0 \tag{2.6}$$

Where T is temperature, H is heating rate, t is time, and T_0 is the initial temperature. Once a mass (or conversion) versus time curve has been generated using the TGA with an experiment, the particular method of determining the activation energy can lead to differing results. This reduction method linearizes the data, and the kinetic parameters can then be determined from the slope and intercept of the resulting linearized equation. Traditional nonisothermal experiments also involve linearizing an equation in some manner and fitting the resulting straight line to obtain activation energy, pre-exponential factor, and reaction order (Abu-Qudais *et al*., 2005). There are some researchers who have pointed out that linearization of an equation is not necessary. A first order global reaction

with an Arrhenius form of the rate constant is often assumed and expressed as shown in Equation 2.7:

$$\frac{\mathrm{dm}}{\mathrm{dt}} = -A \times e^{(-E/R\times T)} \times m \tag{2.7}$$

Where:

T represents the temperature of the sample, A is the pre-exponential factor, and m is the mass. Equation 2.7 can generally be express into Equation 2.8 in terms of nth order equation (n is the reaction order) .

$$\frac{\mathrm{dm}}{\mathrm{dt}} = -A \times e^{(-E/R\times T)} \times \mathrm{m}^{\mathrm{n}} \tag{2.8}$$

The kinetic expressions shown are not ―true‖ explanations of the mechanism but provide useful equations for engineering applications. Traditionally there have been two classes of methods utilizing non-isothermal data to determine the kinetic parameters used, (Popescu, 1998). One method simply requires a linearization of this eqquation by dividing by the mass and then taking the natural log or log10 of both sides.

2.10.2 Kinetic parameters for oil shale

One industry that has relied extensively on TGA work is the oil shale industry where it has been used to determine kinetic parameters for modeling purposes (Shuyuan *et al*., 2001; Abu-Qudais, 2005). TGA experiments are simple in concept but have several difficulties in practice, especially for pyrolysis experiments. Isothermal analysis in principle starts with zero conversion during the heat up period to the experimental temperature and then proceeds with time, but in reality conversion begins during the heating period (Shuyuan *et al*., 2001).

It was pointed out by Campbell that the difficulty of isothermal analysis is the result of the initial heat up period required to reach the isothermal reaction temperature (Shuyuan *et al*., 2001). Non-isothermal analysis avoids the uncertainty of the initial conditions

(Shuyuan *et al*., 2001). Non-isothermal analysis starts with the temperature much lower than the reaction temperature. For example, one possibility is to start at room temperature and heat the sample at a constant and known rate through the temperature region of reaction. Then Equation 2.8 is solved and fit to the mass loss curve. Non-isothermal experiments are generally shorter and have fewer initial condition problems than the isothermal experiments (Abu-Qudais *et al*., 2005). One major problem with the non-isothermal method is the difficulty of the subsequent analysis. The problem arises in determining the solution to Equation 2.8 due to the Arrhenius form. To simplify the solution many researchers have assumed that n (the reaction order) is equal to 1.0 (Abu-Qudais *et al*., 2005). Researchers have also proposed using Equation 2.7 for parallel first-order reactions (Benbouzid and Hafsi, 2008).

Another proposed non-isothermal solution to the global first order equation mentioned by Shuyuan *et al*. (2001) involves the volume of product generated. The model follows a similar form of Equation 2.7 but has numerically different kinetic parameters owing to the difference between a pyrolysis experiment and an oil generation experiment. The Campbell experiment tracks the amount of product created. The process is more of an oil production process at pyrolysis conditions than a pure pyrolysis process. Campbell's approach, which tracks oil generation, differs from the more popular solutions involving conversion or normalized mass used by many researchers.

Despite the fact that a 1st order equation is commonly employed to describe the oil shale pyrolysis process, not all researchers have used a first order model. This attempted to show that the kinetics of oil shale do not follow first order kinetics. However, their conclusion is that global first-order kinetic parameters agree quite well with known data. It is most likely true that there is more than one reaction occurring in the pyrolysis of oil shale, but a first order model seems to describe the process well.

2.10.3 Isothermal and non-isothermal kinetic study

Isothermal condition in kinetic study occurs when a sample is heated to it reaction temperature and retaining the sample which recording it mass against temperature (Aboulkas *et al*., 2011). It is carried out by plotting the rate constant for more than one experiment against temperature inverse on a log plot. The slop and intercept of the graph represent the activation energy and frequency factor respectively (Aboulkas *et al*., 2011). Non-isothermal system involves heating of the sample with respect to time at a constant heating rate. It avoids uncertainty in initial condition, commence with a temperature lower that the reaction temperature (Aboulkas *et al*., 2011).

A (solid) $\longrightarrow$ B (solid) + C (volatile) (2.9)

$$\frac{dm}{dt} = \beta = \frac{dT}{dt} = K(T)f(m) \quad (2.10)$$

Where m is the mass (degree of advance), f(m) and k(T) are function of conversion and temperature respectively. k(T) is the temperature dependent rate of weight loss which was later developed by Arrhenius.

2.10.3.1 Arrhenius method

A first order equation that was developed by Arrhenius which is used to determine the activation energy and pre-exponential factor is shown in equation 2.11:

$$\frac{dm}{dt} = -A\ exp\left(\frac{-E}{RT}\right)M \quad (2.11)$$

Where T is the temperature of the sample, A is the pre-exponential factor, E is the activation energy, R is the rate of the reaction and M is the mass of the substance. The Equation 2.11 will hold for only first order reaction but for nth order reaction, the Equation 2.12 replaces it;

$$\frac{am}{dt} = -A\ exp\left(\frac{-E}{RT}\right)M \quad (2.12)$$

Equation (2.12) can also be change to the Equation 2.13:

$$\ln\left(-\frac{\left\{\frac{dm}{dt}\right\}}{m}\right) = \ln(A) - \frac{E}{RT} \quad (2.13)$$

Comparing equation (2.13) with the equation of a straight line, 1/T is plotted on the abscissa while the equation on the left hand side is plotted on the ordinate. The slope of the straight line given is the activation energy while the intercept is the pre-exponential factor. The above equations are also referring to as differential method. This method has two major limitations which are the derivative have numerically imprecise evaluation and the pre-exponential value is decenticised because it involves logarithm.

2.10.3.2 Kissinger-Akahira-Sunose method (KAS method)

The base equation for KAS method is shown in Equation 2.14:

$$\frac{dx}{f(x)} = \frac{A}{\beta}\exp(-\frac{E}{RT})dt \quad (2.14)$$

The base equation 2.14, is then integrated with boundary condition x=0 and T=To. The expression in Equation 2.15 was then obtained:

$$g(x)= \int_0^x \frac{dx}{f(x)} = \frac{A}{B} = \int_{T0}^{T}(exp\frac{-E}{RT})\,dt = \frac{AE}{\beta R}\,P\,(\frac{E}{RT}) \quad (2.15)$$

This method assumes that A, f(x) and E are independent on T. The KAS method is an approximation of based on Coat-Redfern approximation method shown in Equation 2.16:

$$\ln\frac{\beta}{T2} = \ln\frac{\mathrm{AR}}{\mathrm{Eg(x)}} - \frac{E}{RT} \quad (2.16)$$

Hence the plot of $\frac{\beta}{T2}$ against 1/T for a constant value x would give a straight line graph would slope will depict the activation energy. It is also called integral method.

2.10.3.3 Freidman method

This is a differential isoconversion method based on logarithm which are express in Equation 2.17:

$$\ln\frac{dx}{dt} = \ln\frac{\beta dx}{dT} = \ln\{Af(x)\} - \frac{E}{RT} \quad (2.17)$$

A graph of $\frac{\beta dx}{dT}$ against 1/T is plotted to obtain the activation energy and preexponential factor.

2.10.3.4 Flynn-Wall-Ozawa method

This method is obtained from isoconversion of the integral method. Doyle's approximation was used which approximate

$$\ln P\left(\frac{E}{RT}\right) = -5.331 - 1.052\,\frac{E}{RT} \quad (2.18)$$

Therefore, this can also be express to form Equation 2.19

$$\ln\beta = \ln\frac{AE}{Rg(x)} - 5.331 - 1.052\,\frac{E}{RT} \quad (2.19)$$

From the Equation 2.19, x is a constant and the plot of lnβ against 1/T will give a straight line grapht which the activation energy and pre-exponential factor can be obtain.

2.10.3.5 Coat-Redfern method

$$\ln\frac{g(x)}{T2} = \ln\frac{AR}{\beta E} - \frac{E}{RT} \quad (2.20)$$

Equation 2.20 was obtained by the use of asympototic approximation.

CHAPTER THREE

3.0 MATERIALS AND METHOD

3.1 Experimental Description and Sampling of Raw Materials

The oil shale sample used was collected from the Royal Ceramics Mine in Ahoko in Kogi State. The samples were ground and sieved to a grain size of less than 0.2 mm and dried at 45-50 ^{o}C to constant mass. The raw polyethylene used in this research work was sourced in Minna, Bosso Local Government Area of Niger State which are listed in Table 3.1:

Table 3.1: List of Material and Chemical used

S/N	Chemical	Manufacturer	Source
1	Oil Shale	-	Ahoko
2	Polyethylene (Waste)	-	Bosso
3	Distilled Water	-	WAFT Lab. Minna
4	Ethanol	-	Panlac, Minna
5	Ether	-	WAFT
6	Potassium iodide	-	Panlac, Minna
7	Acetone	-	Panlac, Minna

The list of used equipment, apparatus and manufacturers are shown in Table 3.2, this also shows the model and their source.

Table 3.2: List of Equipment and Apparatus used

S/N	Equipment	Model	Manufacturer	Source
1.	Filter Paper	-	-	WAFT LAB
2.	Weighing Balance	MP300	Citizen	WAFT LAB
3.	Refractometer	-	Gallen Kamp	WAFT LAB
4.	Pycnometer	-	Pyrex England	WAFT LAB
5.	Beaker	-	Pyrex England	WAFT LAB
6.	PH meter	PH 25	REX	WAFT LAB
7.	Measuring Cylinder	Jaytec	Pyrex England	WAFT LAB
8.	Burrete	-	Pyrex England	WAFT LAB
9.	Conical Flask	-	Pyrex England	WAFT LAB
10.	Funnel	-	-	WAFT LAB
11.	Pippette	-	Pyrex England	WAFT LAB

12.	Round Bottom Flask	-	Pyrex England	WAFT LAB
13.	Glass Rod	-	-	WAFT LAB
14.	Thermometer	Deluxe	-	WAFT LAB

3.2 Characterization of the Oil Shale and Polyethylene

3.2.1 Proximate analysis of oil shale and polyethylene samples

The proximate analysis of the oil shale for moisture content and ash content were determined. Volatile matters, fixed Carbon and Total Nitrogen were determined using Pearson method (Pearson, 1976). This was carried out to determine the various components in the sample. Moisture content was determined by weighing 5 g of the samples into petri-dishes. This was transferred to the oven at 105 ^{o}C and left for 24 h. The samples were removed from the oven, transferred into a desiccator and allowed to cool for 15 min before weighing. The loss in weight was determined recorded as moisture content and the percentage moisture was calculated using Equation 3.1.

$$\% \text{ Moisture content} = \frac{\text{Weight loss}}{\text{Weight of Sample}} \times 100 \quad (3.1)$$

The ash content was determined by taking the weight of the crucibles, 2.0 g of the sample was added to each of the crucibles. The crucibles and the samples were placed in the furnace, the temperature was set at 600 ^{o}C for 3 h until the sample were completely roasted. The ash in crucible were removed and placed in a desiccator to cool. The cooled ash and the dishes were re-weighed and percentage of ash was calculated using Equation 3.2.

$$\%\text{Ash} = \frac{\text{Total weight of extracted ash}}{\text{Weight of Sample}} \times 100 \quad (3.2)$$

Total Organic Carbon (TOCs) were determined by weighing 2.0 g of dry oil shale (A) into conical flask, 50 mL of 12.5 mL/L of H_2SO_4 was poured into the conical flask and then the oil shale sample was heated and until it started boiling, it was allowed for 30 min. After which the mixture was filtered and rinsed with cold water, followed by the addition of 50 mL of 25 % sodium hydroxide (NaOH) it again heated and allow to boil for 30 min. It was filtered and rinsed with cold water. The remaining wet sample was placed in the crucible and allowed to dry in the oven for some time. There after the crucible was

reweighed (B) and placed in furnace at 600 ºC for 30 min and reweighed (C). Thus the percentage TOC was calculated using Equation 3.3

$$\%\text{TOC content} = \frac{B-C}{A} \times 100 \quad (3.3)$$

3.2.2 X-Ray diffraction (XRD) of oil shale and polyethylene

The attribute of the oil shale was analyzed using XRD, the shale sample was finely ground homogenously and average bulk composition was determined. The powdered sample was then prepared using the sample preparation block and compressed in the flat sample holder to create a flat, smooth surface that was later mounted on the sample stage in the XRD cabinet. The sample was analyzed using the reflection-transmission spinner stage using the theta-theta settings. 2θ starting position was 4 degrees and ends at 80 degrees with a 2θ step of 0.026261 at 8.67 seconds per step. Tube current was 40 mA and the tension was 45 VA. A Programmable divergent slit was used with a 5 mm width mask and the Gonio Scan was used. The intensity of diffracted X-rays was continuously recorded as the sample and detector rotate through their respective angles. A peak in intensity occurs when the mineral contains lattice planes with d-spacing, appropriate to diffract X-rays at that value of θ. Although each peak consists of two separate reflections ($K\alpha_1$ and $K\alpha_2$), at small values of 2θ the peak locations overlap with $K\alpha_2$ appearing as a hump on the side of $K\alpha_1$. Greater separation occurs at higher values of θ. Typically these combined peaks are treated as one

3.2.3 Scanning electron microscopy (SEM) of Ahoko oil shale

The scanning electron microscopy (SEM) was performed to examine the physical structure change of the samples using SEM model Phenom ProX,by phenomWorld Einhoven, Netherland, The Samples was placed on double adhesive which was on a sample stub, was coated with a sputter coater by quorum technologies model Q150R,with

5 nm of gold. Thereafter it was taken to the chamber of SEM machine where it was viewed via NaVCaM for focusing and little adjustment, it was then transferred to SEM mode.

3.2.4 Fourier transform-infrared spectrophotometer FT-IR of both oil shale and polyethylene samples

The FT-IR spectra of the oil shale and polyethylene were examined to identify the functional groups present in both samples. This was done using a FT-IR machine in NARICT, Zaira. The oil shale and polyethylene were analyzed with spectra measured with 500 to 4000 cm^{-1}. The results obtained were utilized to determine the various functional groups in both samples.

3.2.5 Thermogravimetric analysis of oil Shale, polyethylene and their mixtures

The oil shale, polyethylene and their mixture samples were subjected to thermogravimetric analysis (TGA) in an inert atmosphere of nitrogen. Perkin Elmer TGA 4000 (Netherlands) was used to measure and record the sample mass change with temperature over the course of the pyrolysis reaction. Thermogravimetric curves were obtained at 10 ^{0}C/min between 27 ^{0}C to about 1000 ^{0}C, the precision of reported temperatures was estimated to be ± 27 ^{0}C. Nitrogen gas was used as an inert purge gas to displace air in the pyrolysis zone, thus avoiding unwanted oxidation of the sample. A flow rate of around 60 ml min^{-1} was fed to the system from a point below the sample and a purge time of 60 min (to be sure the air was eliminated from the system and the atmosphere is inert). The balance can hold a maximum of 45 g; therefore, all sample amounts used in this study was noted.

3.2.6 Gas Chromatography and mass spectrometry (GC-MS)

The shale oil sample was analyzed using Agilent technologies 7890A GC and 5977B MSD. The experimental conditions of GC-MS system were as follows: Hp 5-MS capillary standard non-polar column, dimension: 30M, ID: 0.25 mm, Film thickness:

0.25 μm. Flow rate of mobile phase (carrier gas: He) was set at 1.0 ml/min. In the gas chromatography part, temperature programme (oven temperature) was 40 °C raised to 250 °C at 5 °C/min and injection volume was 1 μl. Samples dissolved in methanol were run fully scan at a range of 40-650 m/z.

3.3 Determination of the Yield of Oil

3.3.1 Design of experiment

Response surface methodology (RSM) with five-level-four-factor central composite design (CCD) was applied to optimize that is to maximize production of shale oil from oil shale and polyethylene using DESIGN EXPERT (Version 7.0.0, Stat Ease, Inc., USA) software. In this study two factors to be considered which are oil shale and polyethylene. A total of 13 experiments were conducted separately to obtain experimental responses for percentage yield of shale oil. The independent factors used in this study for pyrolysis of oil shale and

3.3.2 Pyrolysis experiment of ahoko oil shale and polyethylene samples

The pyrolysis experiment of oil shale sample was performed in a 150 ml stainless steel autoclave reactor, with a sweep gas (nitrogen) connection. The autoclave reactor was operated at the pressure of 250 bar. The autoclave reactor was heated externally by an electric furnace and the initial nitrogen gas pressure was 6 bar. The oil shale sample base on the runs was placed in the autoclave reactor; nitrogen steam was introduced into the reactor. The autoclave reactor was heated from room temperature to 500 – 900 ^{o}C at

different heating rate of 5, 10, 15 and 20 °Cmin^{-1} under nitrogen gas pressure and held at this final temperature for 15 min. After the experiment, the autoclave reactor was cooled to the temperature of about 0 °C with an ice-salt bath. The gaseous products were vented and then the reactor contents were filtered to separate solid and liquid parts, the oil obtained was then characterized using FTIR and GC-MS. The same procedure was used for the pyrolysis of the polyethylene sample.

3.3.3 Co-pyrolysis experiment of polyethylene and Ahoko oil shale

The reactor was loaded with 60 g of each sample of the mixture, based on the mixture fractions specified by runs in design expert. The autoclave reactor was connected to the Liebig condenser and water at room temperature was pumped, bottom-up through the condenser using Console drive Masterflex peristaltic pump set at a flow rate of 20 $mLmin^{-1}$. The pyrolyser connected to electrical source was heated at different heating rate of 5, 10, 15 and 20 ^{o}C/min, (Zhao *et al*., 2020). The condensable gases from the pyrolysis process were condensed into liquid and collected in a measuring cylinder to measure the volume of oil produced. The maximum operating temperature was 525 ^{o}C (Demirbas, 2018) and the residence time was 90 mins because the pyrolysis of oil shale and polyethylene can produce fuel at 500 ^{o}C in the reactor according to TGA analysis conducted and the pyrolyser can reach temperature beyond 525 ^{o}C at a residence time of 90 min.

3.3.4 Statistical analysis

Design expert (Version 7.0.0, Stat Ease, Inc., USA) software was used for generating a model equation from the experimental data obtained from the co-pyrolysis of oil shale and polyethylene at maximum temperature of 525 ^{o}C and residence time of 90 min.

Regression analysis was used to fit the model equation, and estimation of the statistical significance of the model was done using analysis of variance (ANOVA).

3.3.5 Optimization of the models

Numerical optimization tool in the Design expert (Version 7.0.0, Stat Ease, Inc., USA) software was applied to optimize the model generated by searching out the factors space from the analysed experimental data for the best trade-offs to achieve a maximum oil yield. The optimization process had the parameters considered include oil shale (A) and polyethylene (B) in the design space to improve chances for finding the best ratio and at maximum yield

CHAPTER FOUR

4.0 RESULTS AND DISCUSSION

4.1 Proximate Analysis of the Oil Shale and Polyethylene samples

The proximate analysis of the oil shale and polyethylene used are shown in Table 4.1, the proximate analysis shows moisture content, ash content volatile matter while the ultimate analysis shows carbon, hydrogen, nitrogen and sulphur contents. The properties of Ahoko oil shale was then compared with other oil shale from Funshun, Hindiuan, Moaming oil shale in China and also Tarfaya oil shale in Morrocco. The results do not show a wide disparity while Ahoko oil shale has high carbon content of 41.2 % which is more than those of China at 13.82 %, 32.888 % and 16.05 % respectively but is lower than that of Morrocco at 57.50 % this may be due to the geological formation of the oil shale. The values obtained for the polyethylene was also compared to the theoretical polythene from literature, it was observed that the value for volatile matter was 77.90 % while that of the polyethylene according to (Aboulkas *et al*., 2008) was 99.6 % for volatile matter and other parameters are shown in Table 4.1.

Table 4.1: Results of Proximate and Ultimate Analysis of Ahoko Oil Shale and Polyethylene

Proximate Analysis (wt%)	Oil Shale	Polyethylene
Volatile matter	46.00	77.90
Ash content	42.50	10.66
Moisture content	4.69	0.17
Fixed Carbon	6.81	12.20
Ultimate Analysis		
C	42.00	84.95
H	3.20	14.20
N	0.29	-
S	2.25	0.59

4.2 Characterization of Ahoko Oil Shale and Polyethylene

The following analysis was carried out on the samples which are thermo-gravimetric analyses (TGA), X-ray diffraction (XRD), Scanning Electron Microscopy (SEM), Fourier transform infrared spectra (FT-IR**)** and Gas Chromatography Mass spectrometry (GCMS).

4.2.1 X-ray Diffraction pattern of the oil shale and polyethylene

4.2.1.1 X-ray diffraction diffractogram of oil shale

The X-ray Diffraction Pattern of oil shale in Figure 4.1 shows the degree and intensity at which each peaks occur as it was giving.

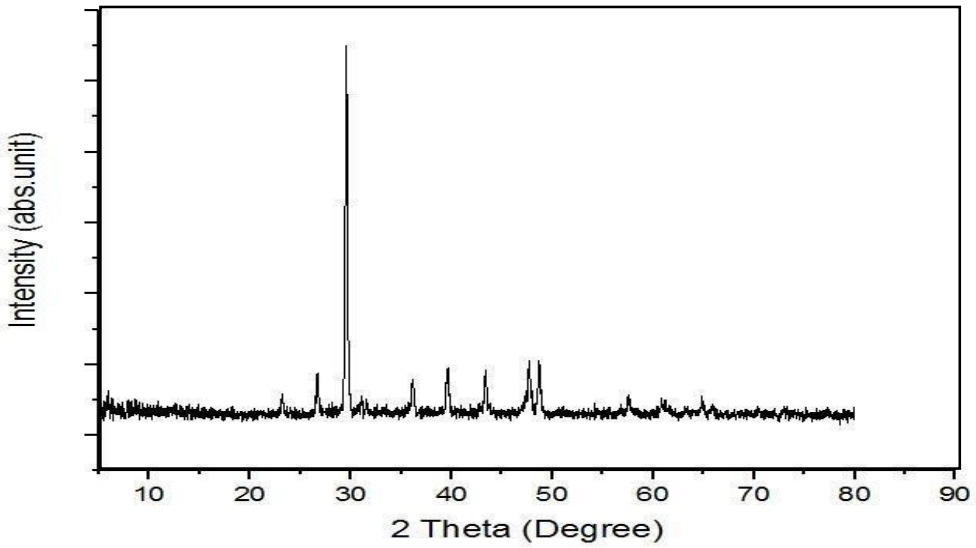

Figure 4.1: XRD Diffractogram of Ahoko Oil Shale

Figure 4.1 shows the XRD pattern of the Ahoko oil shale, it was observed that the peaks of the XRD occur at 23 ^{O}C, 26 ^{O}C, 29.5 ^{O}C, 37 ^{O}C, 40 ^{O}C, 45 ^{O}C, 49 ^{O}C, 50 ^{O}C, and 58 ^{O}C which are also similar to Jordanian oil shale as reported by Bai *et al*. (2015). The little change in their peaks might be as a result of geographical location. It was noted that the XRD peaks of these sample represent the minerals present in the oil shale samples and from the XRD analysis in Figure 4.1 shown the main components of the mineral matter

include; calcite, quartz, apatite and kaolinite. Inside capsules, in addition to organic matter, high aluminum and silicon content was observed suggesting the presence of clay in association with organic matter. The presence of clay minerals in close affinity with kerogen would act as a catalyst during the pyrolysis process. Furthermore, the mineral matter present in oil shale is believed to play an important role in the thermally induced catalytic alteration of kerogen during petroleum formation (Liu *et al*., 2020). FTIR spectrum of each oil shale consists of stretching and bending vibrations from the aliphatic and aromatic groups of kerogen, which overlap with the peaks of minerals such as carbonates, quartz, and clay (Bai *et al*., 2015). The information about the aromatic carbons revealed by the XRD analysis can help us understand the structure of aromatic carbons in kerogens (Wang *et al*., 2014).

4.2.1.2 X-ray diffraction diffractogram of polyethylene

The X-ray Diffraction Pattern of polyethylene in Figure 4.2 shows the degree and intensity at which each peaks occur.

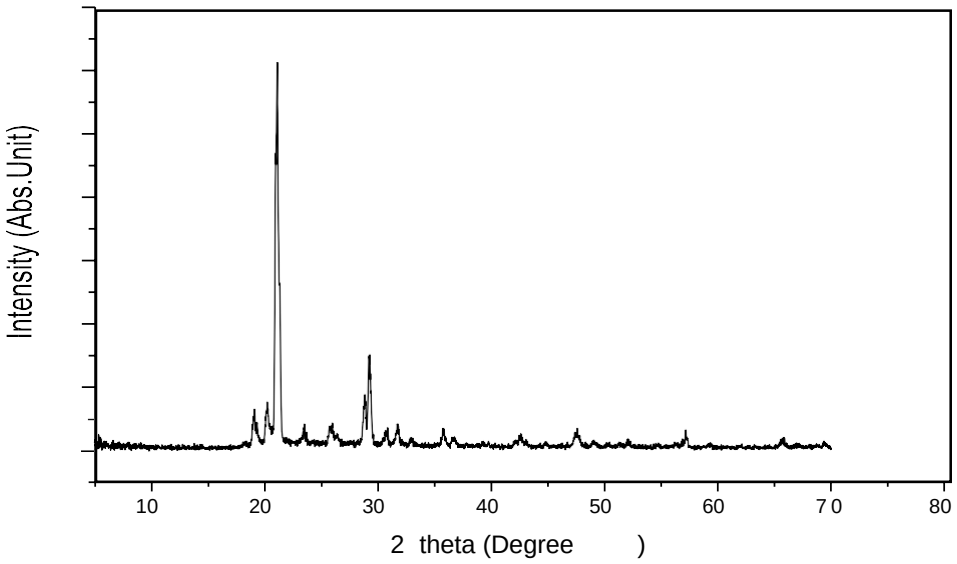

Figure 4.2: XRD Diffractogram of Polyethylene sample

Figure 4.2 shows the XRD pattern of Polyethylene, it was observed from the figure that the highest peaks of the XRD occur at 21^{o} while the XRD of polyethylene getting

according (Wang *et al*., 2018) was at 23 ^{o}. The presence of the amorphous component is clearly apparent, as indicated by the broad in rang 4 to19. The presence of the peaked feature at about 19.50 in Figure 4.2 attributed to a minor amount of monoclinic polyethylene. The corresponding statistical weight was sub-sequent reduced during the refinement and finally set to unit weight at the last cycle without any significant displacement of the fractional coordinates of carbon and hydrogen atoms. This was done to avoid divergence or convergence toward false it was observed that which represents the element or minerals present in the sample.

4.2.3 Scanning electron microscopy (SEM) of Ahoko oil shale

The result of scanning electron microscopy (SEM) which was performed, to examine the physical structure change of sample as show in Figure 4.3.

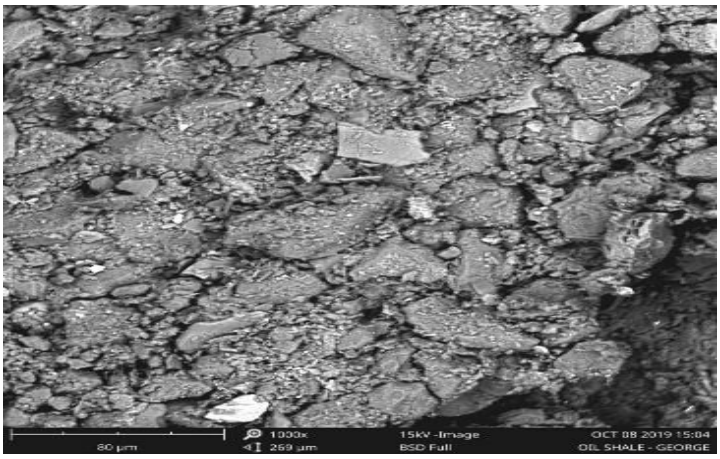

Figure 4.3: The SEM Morphology of Ahoko Oil Shale Sample

Figure 4.3 show the imaged sample at a range of magnifications to characterize the morphology of the oil shale rock fabric and the distribution of minerals and organic material. Compounds with a low mean atomic number such as organic matter appears dark (black), and minerals with a high mean atomic number such as pyrite appear light (white) in standard grayscale digital images. Although the intensity of organic matter is very low, void spaces, such as pores and fractures, exhibit even lower intensity, allowing

for pore identification in images of shales. The SEM of the Ahoko oil shale sample reveals the structure and distribution of organic matter inorganic minerals and porosity at the micron to nanoscale. Domains of darker gray levels represent organic matter, primarily as kerogen with a predominantly amorphous structure. The brighter gray level reflects higher density carbonate phases, and the brightest gray level represents pyrite.

4.2.4 The FTIR spectrum of Ahoko oil shale and polyethylene samples.

The FTIR pattern of the Ahoko oil shale and polyethylene samples are shown in Figure 4.4 and 4.5. Table 4.2 which represents the infrared absorption spectrum bands of kerogen functional groups and pyrolysis products. Therefore, Table 4.2 explains better the FTIR pattern which shows the functional group of each wave number.

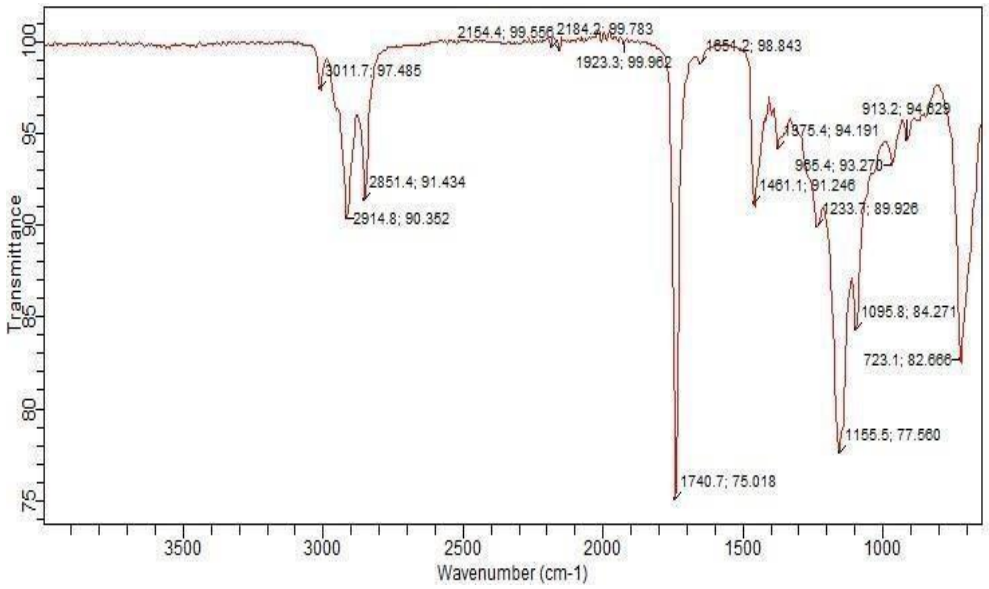

Figure 4.4: FTIR spectrum of the oil shale sample before pyrolysis

From Figure 4.4 shows FTIR spectrum of Ahoko oil shale samples before prolysis. As can be seen, this sample exhibits a complex spectrum formed by the superposition of bands due to the organic matter and to the mineral matrix. Therefore, the organic matter was identified by the main unsaturated and saturated aliphatic C–H absorption bands around 2914, 2851 and 1461 cm^{-1} these also revealing the dominance of sapropelic kerogen. The existence of aromatic compounds in Figure 4.4, show the eligibility because

of the absence of their characteristic band at about 3000 cm^{-1} (Quan *et al*., 2016). On the other side, the high intensity occurrence at 1740 cm^{-1} for Figure 4.4 indicates the possible presence of carbonyl kinds (Liu *et al*., 2020). Other absorption bands which appear around 1630 cm^{-1} were attributed to internal water molecules of mineral clays. The multitude of bands observed in the region 1125–420 cm^{-1} were assigned to different vibration Si–O modes of quartz (Quan *et al*., 2016). The presence of carbonate absorption bands ($CO3^{2-}$) at 1452 cm^{-1} confirms the results of the XRD analysis described above. The FTIR analysis results show that Ahoko oil shale contains organic matter with dominance of aliphatic chains (type 1 kerogen).

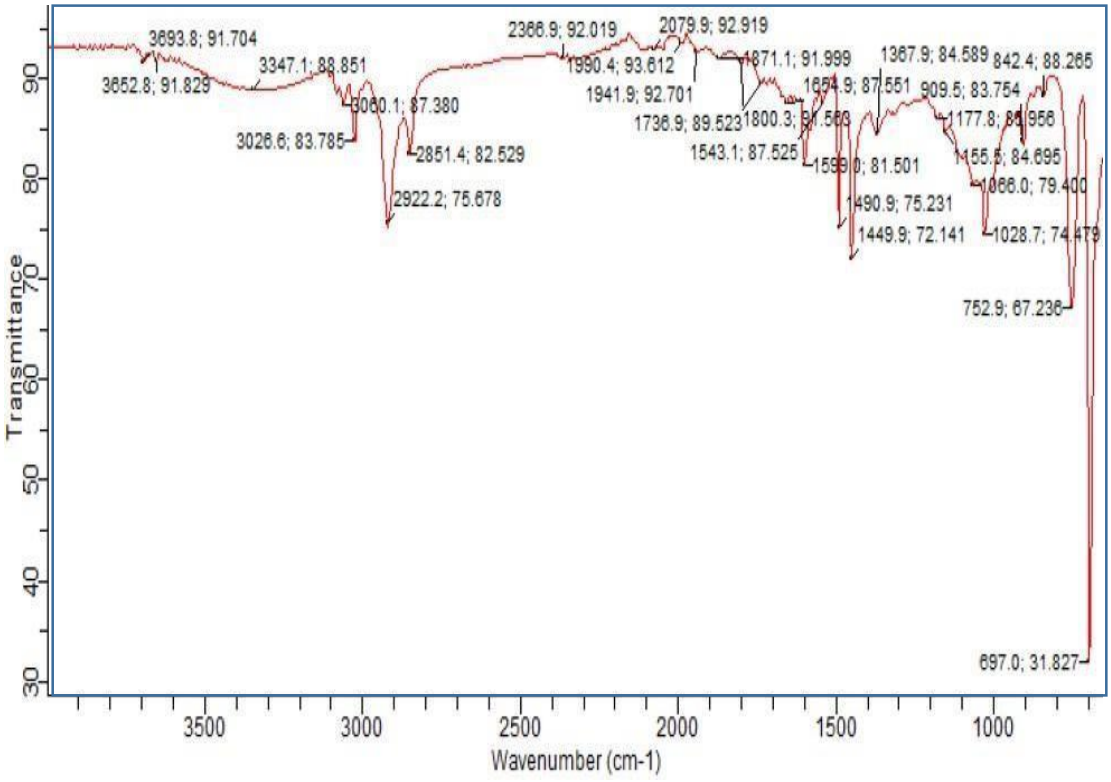

Figure 4.5: FTIR spectrum of polyethylene sample before pyrolysis

Figure 4.5, shows FTIR spectrum of polyethylene samples. As shown, this sample exhibits the same spectrum of bands due to their polymer structure attained. The characteristic polyethylene absorbance bands are located at 2914 cm^{-1}, 2847 cm^{-1}, 1470 cm^{-1}, and 718cm^{-1}. The underline absorbance bands are used to identify and quantify the

presence of Polyethylene. The peaks at 1470 cm $^{-1}$ and 718 cm $^{-1}$ were used to qualify and quantify the presence of Polyethylene, Rocking vibration peaks of methylene were also noted in the spectrum (Zahid *et al*., 2016).

Table 4.2: Some FTIR bands of kerogen functional groups and pyrolysis products

Pyrolysis product/Functional group	Wave number, cm–1
H_2O	4000–3100, 1900–1300
CH_4	3014
CO_2	2400–2240, 780–560
CO	2240–2060
O–H	stretching 4000–3100
CH_2, CH_3 stretching	2926-2922, 2896-2890 (Aliphatic asymmetric)
C=O stretching	1850–1600 (carbonyl compounds: ketone acid, aldehyde, ester, acyl amide, acyl chloride estolide, etc.)
CH	1500–1300 (saturated aliphatic hydrocarbons), 1300–900 (unsaturated aliphatic hydrocarbons), 750–400 (aromatic rings)
C–H stretching	3100–3000 (adjacent to a double bond or aromatic ring), 3000– 2800 (aliphatic compounds)

The absorbance strength at any wave number in the FTIR spectrum region of the tested kerogen samples can be obtained through that which reflects the concentration of substances (functional groups) in kerogen Wang *et al*. (2014). Figure 4.4 and 4.5, shows the infrared absorption spectra of the microstructure of kerogen samples. Based on FTIR and quantum theory Wang *et al*., 2014, the infrared spectra of the samples were divided into the following three regions: aliphatic hydrocarbons CHx stretching vibration, aromatic (–Ar) outer surface deformation and vibration, and other oxygencontaining hetero-atom stretching vibrations.

4.2.5 Thermo-gravimetric analysis (TGA) of oil shale, polyethylene and mixture

Thermo-gravimetric Analysis (TGA) at different heating rate of oil shale, Polyethylene and mixtures are shown in Figure 4.6, 4.7 and 4.8. These TGAs/DTAs show three mass losses of the samples and at the same time inform the choice of temperature ranges at which pyrolysis should take place**.**

4.2.5.1 Thermo-gravimetric analysis (TGA) of oil shale

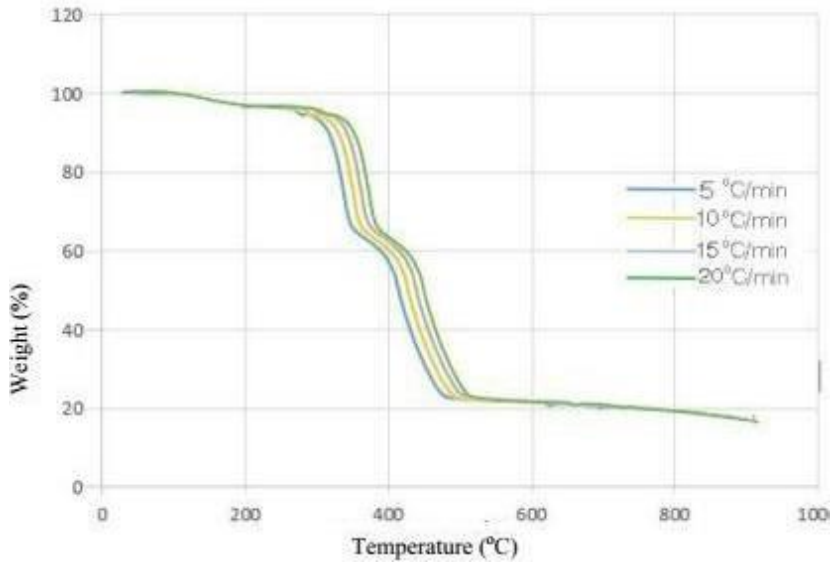

Figure 4.6: Thermogravimetric analysis of Ahoko oil shale sample

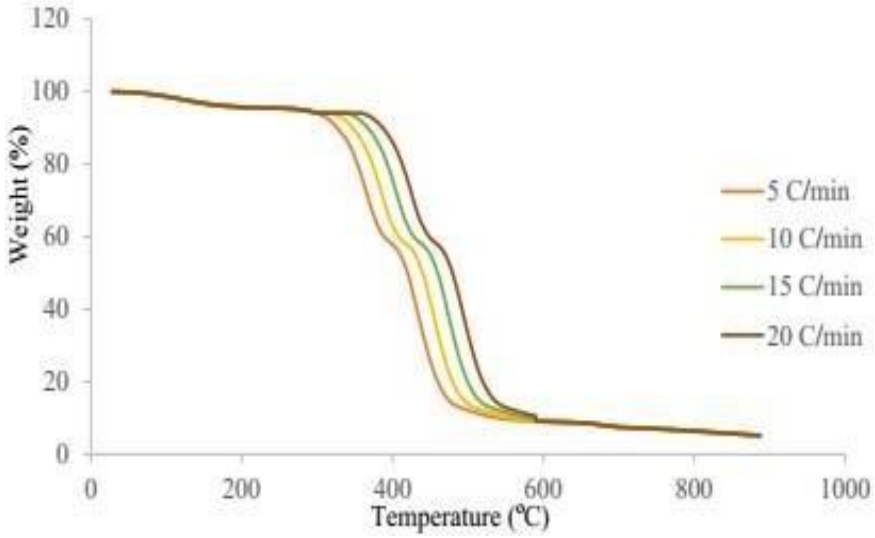

Figure 4.7: Thermogravimetric analysis of polyethylene shale sample

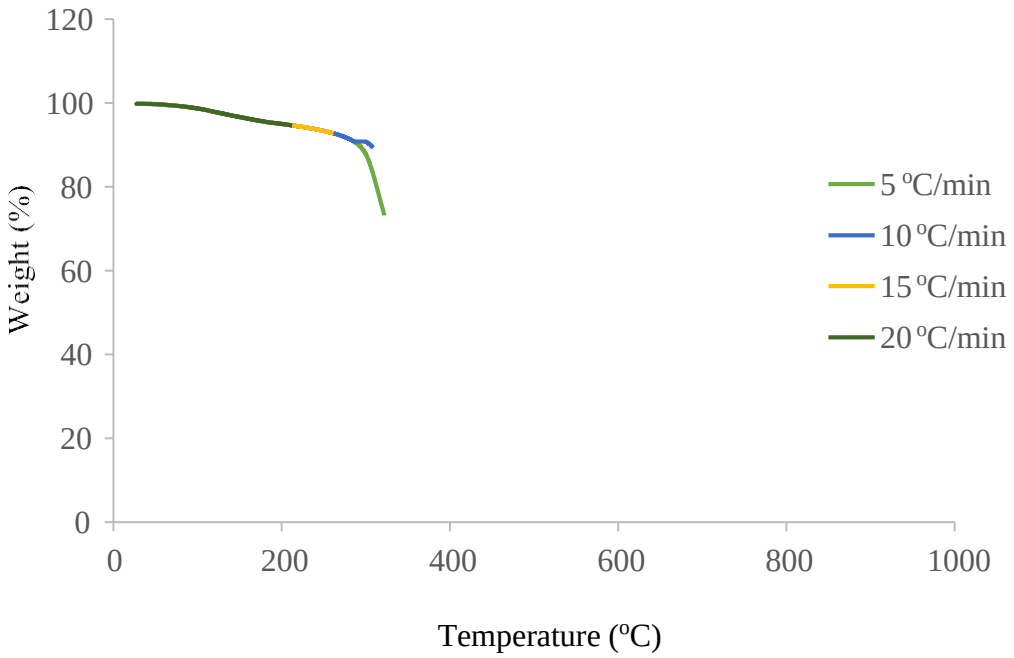

Figure 4.8: Thermogravimetric analysis of mixture of oil shale and polyethylene sample

Figure 4.6, 4.7 and 4.8 show the thermal behavior of Ahoko oil shale, polyethylene and their mixture respectively. The Thermo-Gravimetric Analysis profiles show three mass losses at different heating rate. At temperature less than 300 °C, it was observed from Figure 4.6 and Figure 4.7 that the mass losses of the samples were about 5 % while that of Figure 4.7 was also 5 %, and for Figure 4.8, it was 4 %. These corresponded to endothermic peak attributed to the removal of moisture as well as water molecules associated with the mineral matrix. The second and main mass loss occurring between 300 and 525 °C for Figure 4.6, while that of mixture was between 300 to 500 °C and these corresponds to the pyrolysis of kerogen present in oil shale to form oil, gas and residual carbon (Zhao and Yang, 2020). This second stage was considered as the important pyrolysis step in processing oil shale. The temperature corresponding to the maximum pyrolysis rate and evaluated at 525 °C was similar to Kentucky and Green River oil shales (Demirbas, 2016). According to the literature, low maximum decomposition temperature informs about the nature of organic materials and probably indicates a high kerogen reactivity in agreement with type I kerogen (Demirbas, 2016). In the temperature range

between 550 and 650 °C, the low mass loss observed was attributed assigned to the decomposition of pyrite contained in Ahoko oil shale. The result of Independent Factors used for CCD in pyrolysis of oil shale and polyethylene in order to know mass fraction of each the variables are stated in Table 4.3.

Table 4.3: Independent Factors used for CCD in pyrolysis of oil shale and polyethylene

Variables	Lower	Upper
Oil shale	10	40
Polyethylene	10	40

4.3 Pyrolysis Oil yield at varying Mixture Composition

The responses (quantity of oil yield) recorded from the experimental runs are shown in Table 4.4. The experimental runs 2 which composed of 30g of oil shale and 15.86 of polyethylene produced the lowest pyrolysis oil yield. The highest oil yield was obtained at experimental run 1, 4, 7, 9 and 11 when the mixture composition was 50% oil shale and 50% polyethylene. The low oil yield from components with high proportion of the oil shale could be linked to the chemical composition of the oil shale which was also determined through the result of ultimate analysis carried out. The polyethylene composed of short chain hydrocarbon whose thermal degradation results in the production of liquid product, which was stable at room temperature. Therefore, the increasing quantities of oil shale and polyethylene in the mixture results into increase in the production of pyrolysis oil compare to individual oil yield. These observations agree with the studies by Gersten *et al*. (2000). The mixture with high percentage of oil shale and less polyethylene produced thick and dark viscous pyrolysis oil. The appearance of the pyrolysis oil produced from the mixture composed of equal percentage of each component (oil shale and polyethylene), is dark coloured with some quantity of sludge at the base.

Table 4.4: Optimization of Pyrolysis oil yield at varying mixture composition

Standard Order	Actual Value	Predicted Value	Residual
1	49.59	49.59	-6.490E-004
2	29.47	32.21	-2.74
3	47.16	45.83	2.33
4	49.59	49.59	-6.490E-004
5	31.40	33.36	-1.96
6	39.18	37.34	1.84
7	49.59	49.49	-6.490E004
8	31.40	33.36	-1.96
9	49.59	49.59	-6.490E-004
10	35.20	36.08	-1.12
11	49.59	49.59	-6.490E-004
12	31.40	30.39	1.
13	45.97	44.86	1.11

4.3.1 Statistical analysis of pyrolysis of oil shale and polyethylene

4.3.1.1 *Analysis of variance (ANOVA) for the* model

The model generated is also supported by the analysis of variance (ANOVA), the model F-value of 39.2 at the p-values <0.0001 implied that the model is statistically significant. The high F-value implied that the model significantly represents the variation that exists in the co-pyrolysis of oil shale and polyethylene with respect to the oil yield and the p-value implied the model terms probably have a real effect on the oil yield. The F-value of lack of fit was 1.0. Hence, the Lack of Fit is not significant relative to the pure error and the model can be said to fit the data within the observed replicate variation. The non-significance of the lack-of-fit indicated the model is appropriate for use as a predictor of the oil yield from the co-pyrolysis. The Fit statistics that showed the evaluation of the fitness of the model is shown in Table 4.6.

Table 4.5: Analysis of Variance of the Pyrolysis of Oil Shale and Polyethylene

Source	Sum of Square	Degree of Freedom	Mean Square	F Value	p-value Prob > F
Model	678.27	5	135.65	36.3	0.0001
A- Oil Shale	291.12	1	291.12	7.79	0.0001
B- Polyethylene	374.62	1	374.62	10.03	0.0001
AB	1	17.06	0.46	0.5210	
A^2	1	293.82	7.86	0.0264	
B^2	1	193.85	5.19	0.00568	
Residual	261.55	7	37.36		
Lack of Fit	261.55	3	87.18	1	
Pure Error	0.000	4	0.000		
Cor Total	939.83	12			

From Table 4.6 the response (oil yield), the value of determination coefficient (R2 = 0.9217) indicates that the model is sufficient to describe the process and the sample variation of 92.17 % for pyrolysis oil yield is attributed to the independent variables and only 7.832 % of the total variation could not be explained by the model. The value of adjusted determination coefficient (Adj R2 = 0.9329) is also very high to advocate for a high significance of the model. The Predicted R^2 was 0.9790 and a difference of 0.0459 which is less than 0.2 (< 0.2) from the adjusted R^2, shows a reasonable agreement. In addition, for adequate precision, which measures the signal to noise ratio, a value of 15.84 was observed. This value ultimately is higher than a ratio of 4 and indicates an adequate signal; hence, the model can be used to navigate the design space.

Table 4.6: Fit Statistics

Std. Dev.	Mean	C.V. %	R^2	Adjusted R^2	Predicted R^2	Adeq Precision
6.11	42.34	14.44	0.9217	0.9329	0.9790	0.1584

4.3.1.2 Model equation and coefficients in terms of coded factors

The model equation generated in terms of coded factors to predict oil yield and the relative impact of each factor on the oil yield below. Components A (oil shale), B (polyethylene), had relative positive impact on pyrolysis oil recovery from the copyrolysis of mixed

materials. While the non-linear blending AB (oil shale × polyethylene) had relative

positive impacts on pyrolysis oil yield. Table 4.10 shows the statistical information of the components in the mixtures. The coefficient estimate reflects the expected change in response per unit change in variable value, when all other factors are considered fixed. The variance inflation factors (VIF) for the variables are between 2.65 for all the factors. This implied a moderately correlated relationship between the predicting variables; hence the regression results gotten from the model is reliable. Although the responses with respect to linear blending of the components have been established by the coefficient estimate, the p-values establish their statistical significance. The variables A, B representing oil shale and polyethylene respectively and connoting their linear relationship with the oil yield are highly statistically significant with their p-values less than 0.0001. The linear blending between A and B (oil shale × polyethylene) is also statistically significant. The model results endorse the tendency of the presence of polyethylene in the components to enhance the recovery of pyrolysis oil from the pyrolysis of mixture.

Oil Yield = 42.57 + 14.73A +16.71B - 4.65AB - 14.63A^2 - 11.8B

Table 4.7: Coefficients in Terms of Coded Factors

Factor	Coefficient Estimate	Df	Standard Error	95 % CI Low	95 % CI High	VIF
Intercept	42.57	1	2.72	36.13	49.01	
A-Oil Shale	14.73	1	5.28	2.25	27.21	2.65
B-Polythylene	16.71	1	5.28	4.23	29.19	2.65
AB	1	6.88	-20.91	11,61	2.00	
A^2	1			-2.29	2.17	
B^2	1	5.22	-24.21	0.45	2.17	

Table 4.8: Result optimazation of oil shale and polyethylene and their response yield

Standard Order	Factor 1A:Oil Shale	Factor 2B: Polyethylene	Yield %	
1	100 %	0 %	19.69	A
2	0 %	100 %	25.61	B
3	30.00	30.00	49.59	C
4	30.00	15.86	29.47	D
5	30.00	44.14	47.16	E
6	15.86	30.00	31.40	F
7	20.00	40.00	39.18	G
8	40.00	20.00	35.20	H
9	44.14	30.00	45.97	I

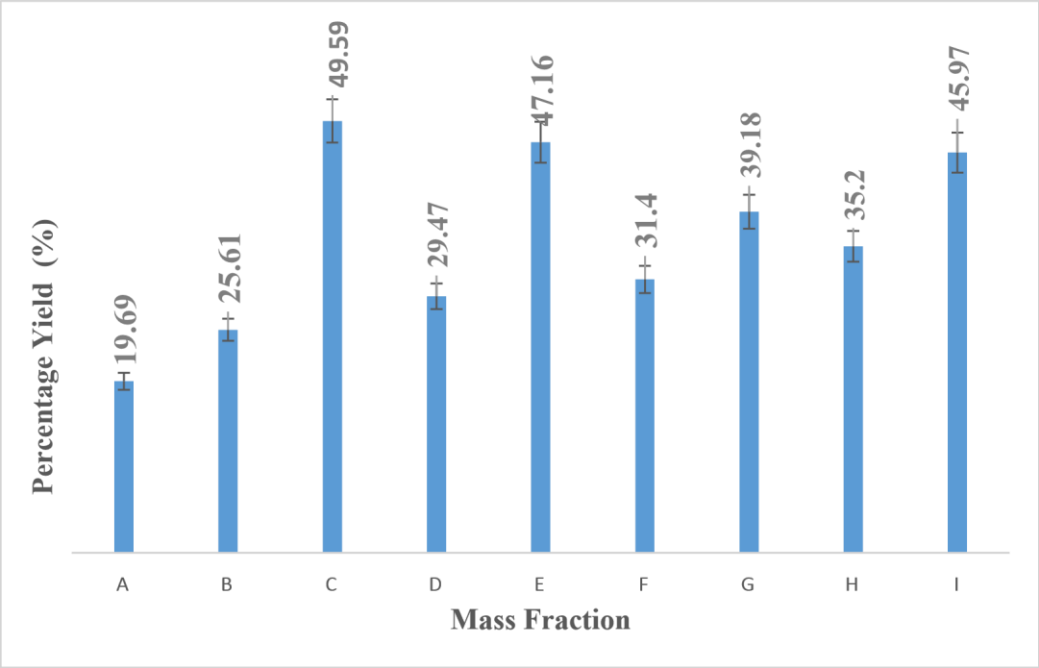

Figure 4.9: Percent products yield (Oil) for at different mixture ratios for the copyrolysis of Oil shale and polyethylene at 525 ^{o}C and 90 min

The goal was set to optimize the compositions of oil shale and polyethylene to achieve maximum pyrolysis oil yield. The numerical optimization result generated based on 99.99 % desirability is at mixture ratio 0.5 oil shale: 0.5 polyethylene. Figure 4.9 shows the plot of percent products yield oil these illustrating the linear blending behavior of the oil shale and polyethylene materials samples at optimum mixture compositions for the oil yield was 49.59 % at 525 ^{o}C and 90 min. The corresponding increase in percentage of oil shale

to polyethylene at mixture ratio of 0.6 to 0.4 respectively led to decrease in oil yield calculated to be 45.97 %. It was also observed that further increase in polyethylene to oil shale at mixture ratio 0.6 to 0.4 respectively, led to slight decrease in oil yield calculated to be 47.16 % when compared to the optimum oil yield which was 49.59 %. The predicted optimum oil yield however, was skewed towards the higher composition of oil shale in the mixture. This observation could be attributed to the shorter hydrocarbon chain produced by oil shale, and long aliphatic hydrocarbon chain produced by the degradation of polyethylene (Vijayakumar and Sebastian, 2018)

4.4 Fourier Transform Infrared Spectra (FT-IR) Analysis of Pyrolysis of Kerogen Samples

From Figure 4.10, it was observed that the FTIR is a suitable technique to examine compositional and structural changes of pyrolysis oils. In addition, several structural alterations or the formation of new entities can also be recognized from their corresponding effect on the FTIR spectrum. Because of the chemical complexity of pyrolysis oil samples, it is difficult to obtain quantitative results from FTIR spectra. The FTIR spectrums of the kerogen obtained by pyrolysis and co-pyrolysis are given in Figure 4.10. The FTIR spectrum of the kerogen obtained from the co-pyrolysis of the oil shale to polyethylene for Figure 4.10 was closely resembled to that obtained from

Polyethylene alone rather than that from the oil shale. The presence of peaks between 3011-3000, 2914-2850 cm^{-1} and the peak in the region from 1350 to 1500 cm^{-1} was due to the C–H bonds indicate the presence of aliphatic groups. The absorbance peaks between 1575 and 1675 cm^{-1} also indicate the presence of olefinic and aromatic compounds. The intense absorption band at 888 cm^{-1} may be assigned to the characteristic vibrational mode of the out-of-plane C–H bending in alkenes. The broad peak around 3473 cm^{-1} as in the case of tar from lignite pyrolysis can be attributed to the O–H

stretching vibrations indicating the presence of phenols and alcohols. The oil obtained in form of kerogen from the co-pyrolysis are characterized by the significant decrease of bands of aromatic, hydroxyl and carbonyl groups and the significant increase of aliphatic groups compared with the oils obtained by pyrolysis of oil shale showed in Figure 10. The possible reason might be related to the hydrogen content of the polyethylene. This is further evidence that polyethylene acts as a hydrogenation medium for the oil shale product under the experimental conditions studied (Shao *et* al., 2008).

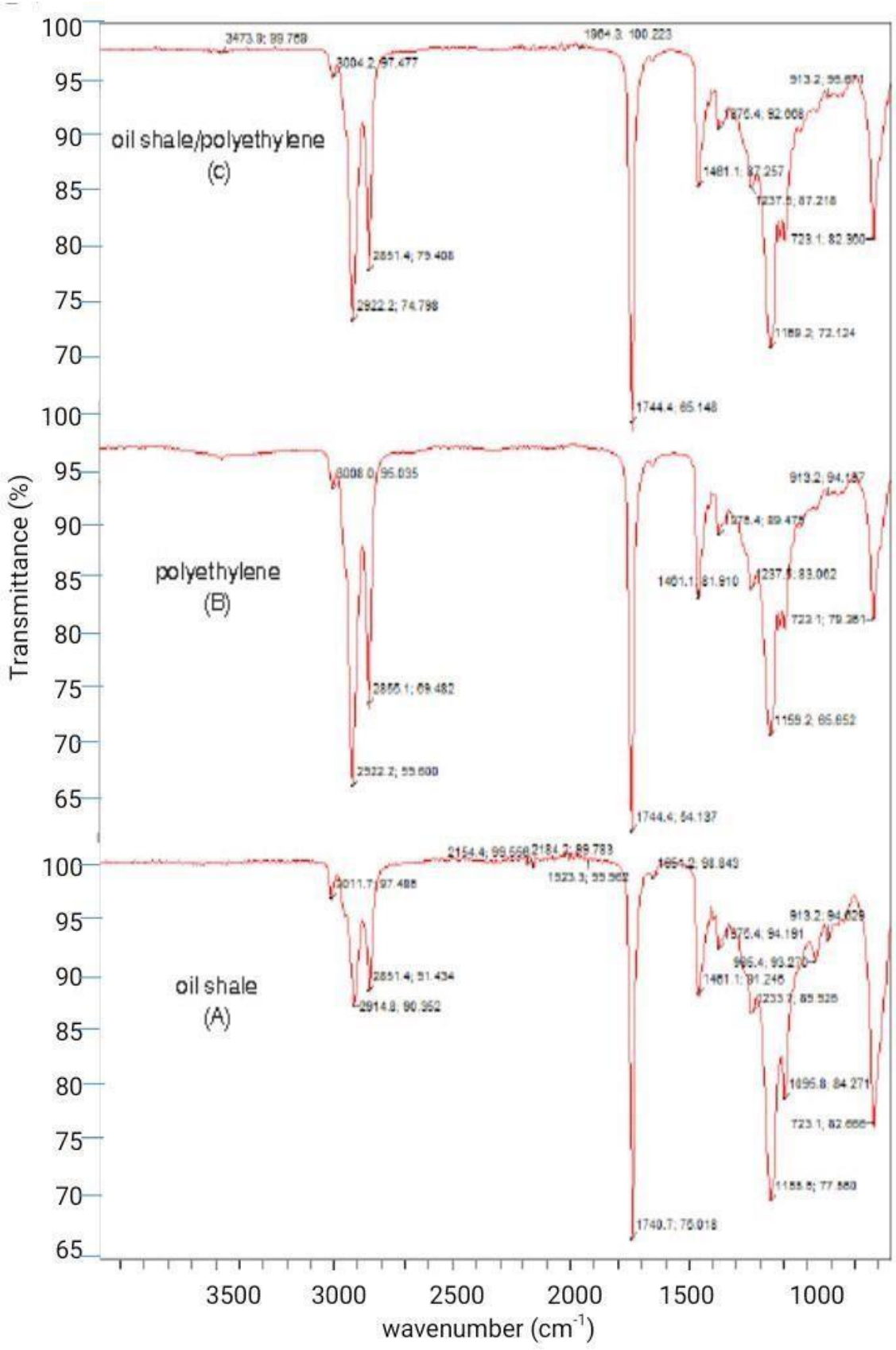

Figure 4.10: FT-IR Analysis of the oil obtained by Pyrolysis and Co-pyrolysis of Ahoko oil shale, Polyethylene and Mixture Samples

4.5 GCMS Analysis of Pyrolysis and Co-pyrolysis of Oils

Mass spectrometry (MS) and gas chromatography (GC) were used to collect chemical structural data and confirm which reaction was indeed the organic reaction on the aforementioned kinetic scheme. Table 4.10 is a table of selected identified peak for the gas chromatographs of the tars generated in the Kerogen.

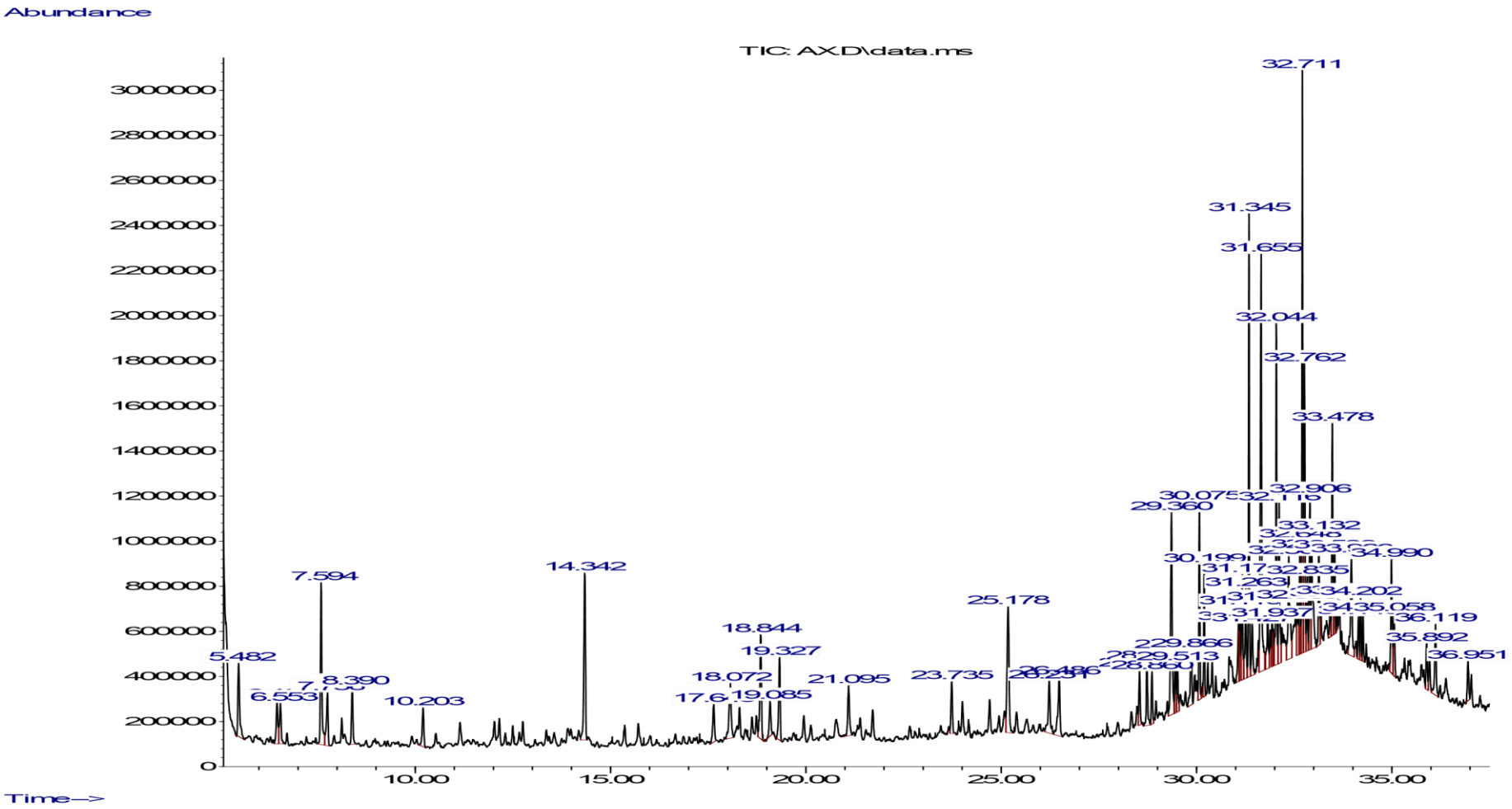

Figure 4.11: shows the GCMS Analysis of kerogen from Ahoko oil shale.

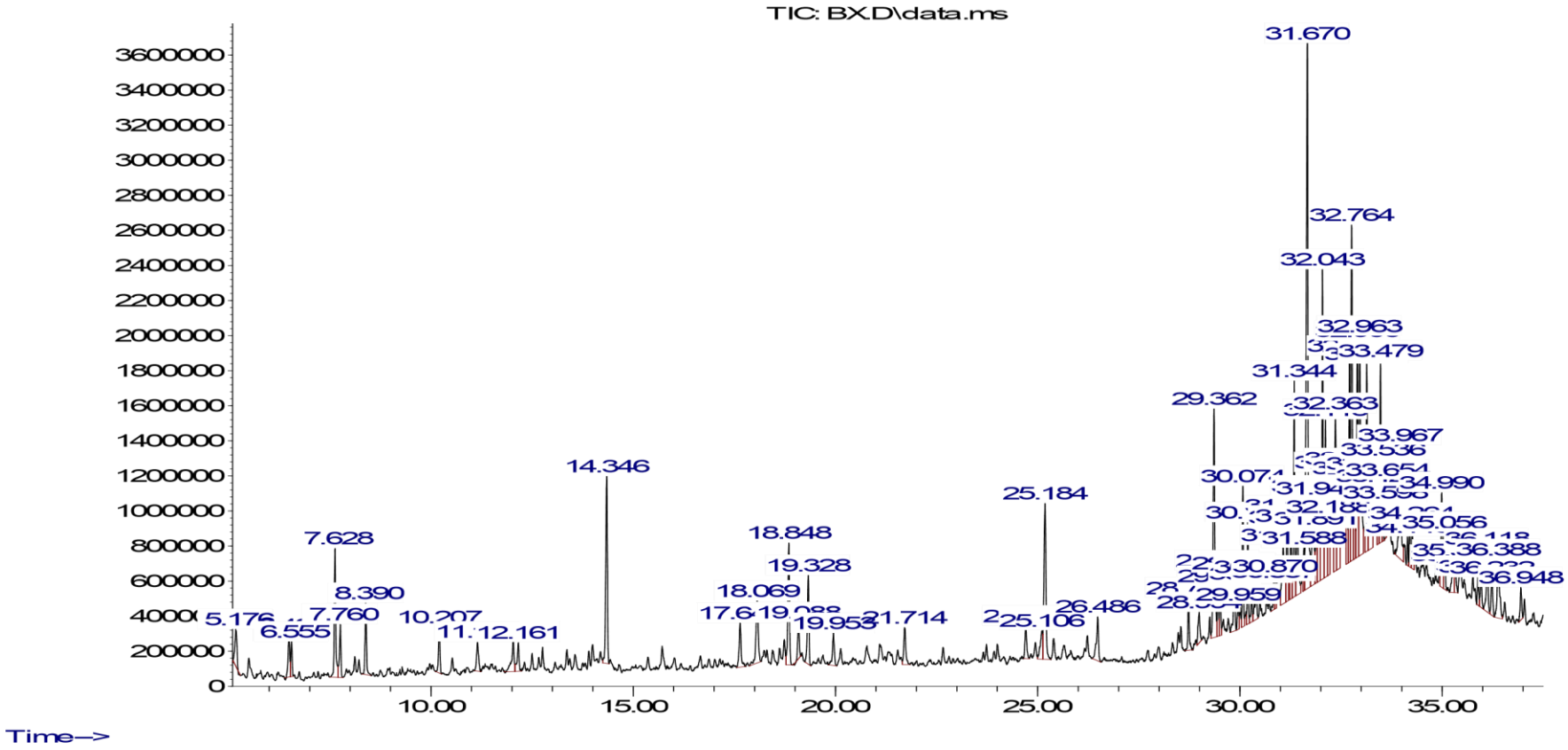

Figure 4.12: shows the GCMS Analysis of polyethylene

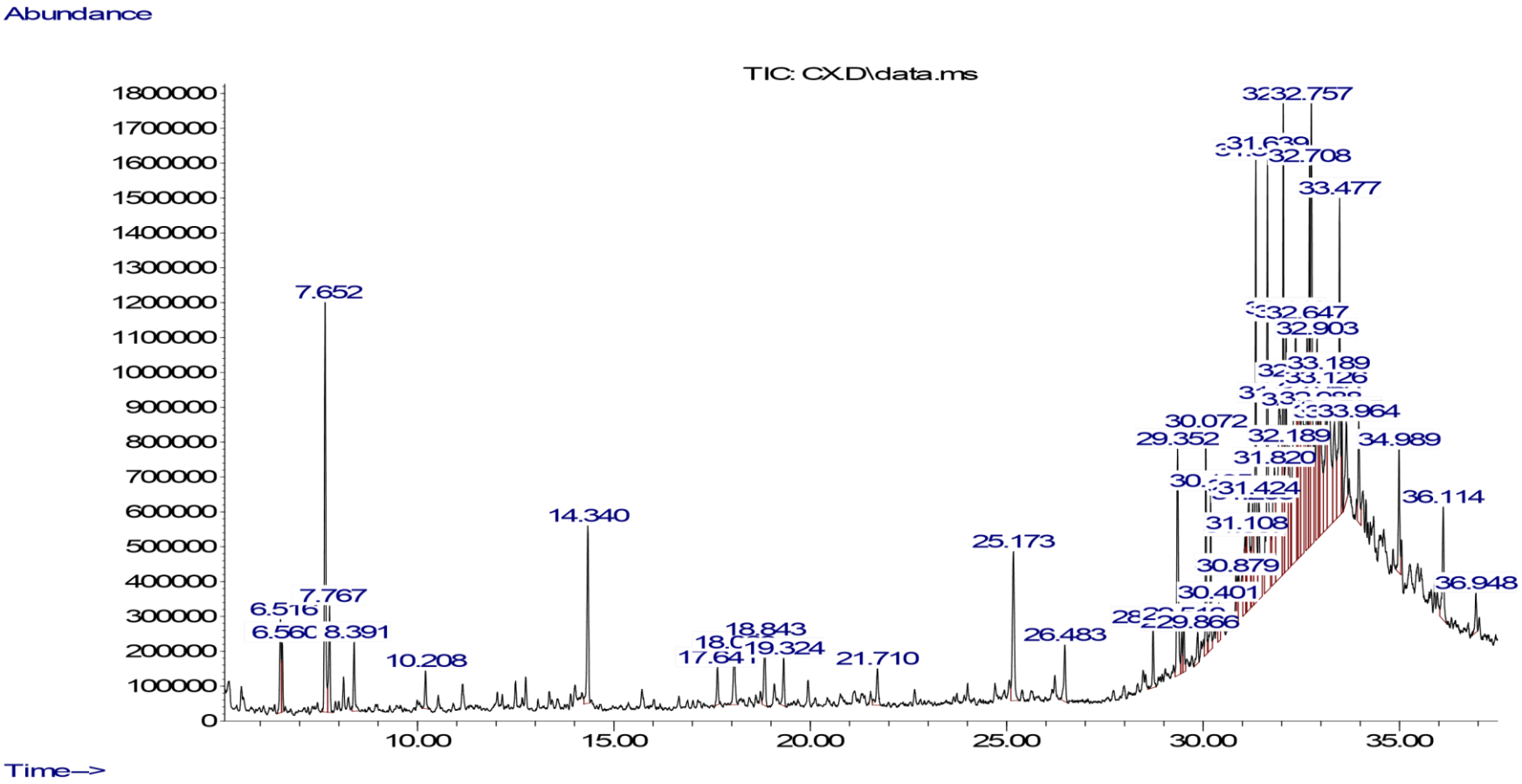

Figure 4.13: shows GCMS Analysis of Kerogen from oil shale and Polyethylene

Table 4.9: Selected Identified Peaks from Figure 4.11, 4.12 and 4.13

Time (min)	Compound	Time (min)	Compound
4.54	Cyclopentanone	19.30	2tridecanone
5.03	1-octene	19.46	pentadecene
5.28	octane	19.63	pentadecane
6.94	2-methylcyclopenatnone	21.10	1hexadecene
7.31	1-nonene	21.26	hexadecane
7.57	nonane	22.66	heptadecene
8.40	trans-2-none-ol	22.81	heptadecane
8.61	4-isopropyl heptanes	22.96	Pristine
		24.13	1octadecene
8.85	phenol	24.26	octadecane
9.22 2	-octanone	25.53 1	-nonadecene
9.62 1	-decene	25.65	nonadecane
9.87	decane	26.86 1	-eicosene
11.83	1-undecane	26.97	Eicosane
12.06	undecane	28.13 1	-henicosene
13.62 2	-decanone	28.23	henicosane
13.91	1-dodecene	29.34	1docosene
14.14	dodecane	29.43	docosane
15.63 2	-undecanone	30.54 1	-tricosene
15.88	1tridecene	30.64	tricosane
16.00	trans-2-tridecanal	31.86 1	-tetracosene
16.09	tridecane	31.97	tetracosane
17.73	1-tetradecene		

GC-MS analysis results of the oil obtained during pyrolysis of the polyethylene and oil shale at 550 ^{o}C and from co-pyrolysis of polyethylene and oil shale mixture at optimum condition at 550 ^{o}C are shown in Figure 4.11. Also individual GC-MS of each sample were conducted and then compare. A significant increase in both alkane and alkene fractions of the polyethylene /oil shale mixtures comparing the results obtained from individual oil shale pyrolysis are observed. Polyethylene addition to oil shale promotes the transfer of hydrogen and free radicals. Oil shale is also considered to be hydrogen donor thus the transfer reactions stabilizes the free radicals produced from the polyalkenes serve as a consequence amount of nalkanes in the tar is increased (Aboulkas *et al*., 2012). Stabilization of radicals proceeds during the pyrolysis process and n-alkenes are formed, this further evidences the presence of interaction between the two sample components.

The chromatogram also shows that the distribution of paraffinic compounds of oil shale ranging from C12 to C26, while for the polyethylene it is between C10 and C24 (with C17 and C19 in trace amounts and absence of C21 and C23). In the case of co-pyrolysis, the chromatogram shows a significant increase in long chain compounds. The distribution in this case is ranging from C9 to C32, indicating, that the oil obtained by co-pyrolysis contains more long chain hydrocarbons. This is due to the polyethylene addition that promotes the formation of saturated hydrocarbons as stated before and similar results were reported by (Aboulkas *et al*., 2012).

4.6 Kinetic Analysis

Pyrolysis reaction parameters are helpful to understand the microscopic reactions that occur during thermal degradation. In particular, activation energy, the minimum energy required by a chemical reaction to occur, has a critical significance for the evaluation of the kinetic scheme of thermal degradation processes. For calculation of activation energy, different values of the conversion degree base on optimum yield were considered and the activation energy was obtained from the slopes of the linear regression lines for the Arrhenius and FWO methods.

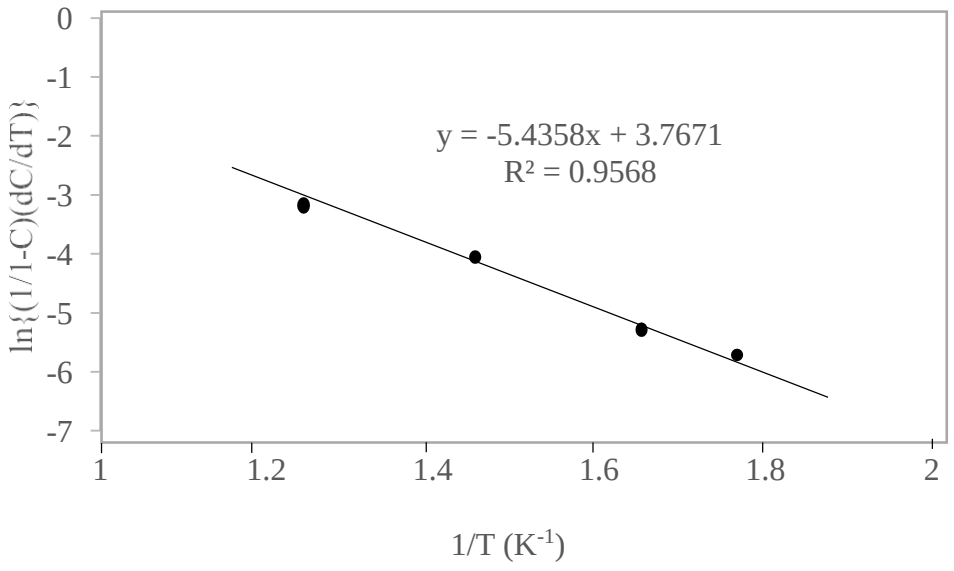

Figure 4.14: Activation Energy of Oil Shale using Arrhenius method

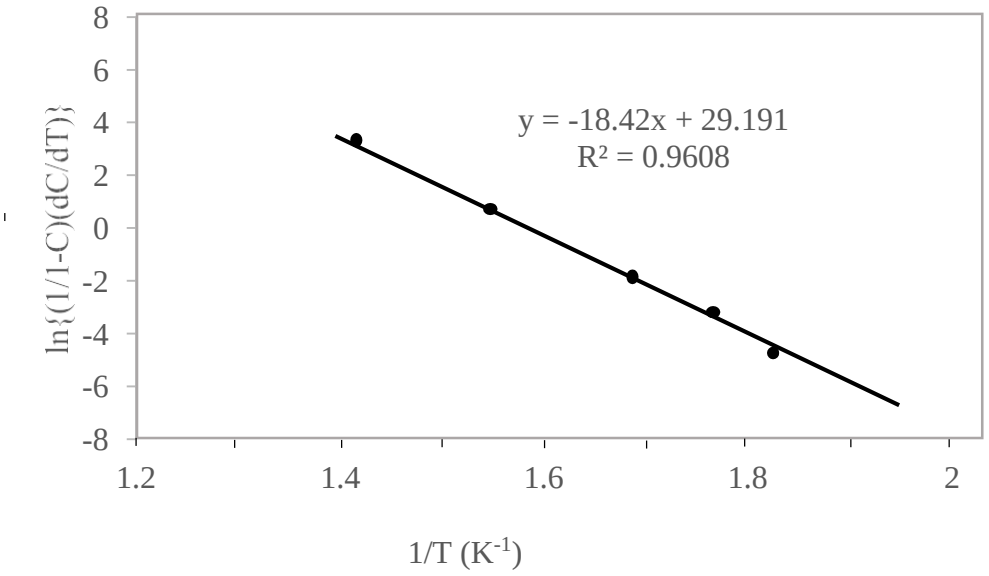

Figure 4.15: Activation Energy of Polyethylene using Arrhenius method

TGA of thermal decomposition of polyethylene shows that degradation starts at about 180 ºC and ends at about 580 ºC. The activation energy of polyethylene was calculated using Arrhenius method to be 153.14 kJ/mol, literature shows that (Gorlov *et al*., 2007), calculated the activation energy of polyethylene to be 123 kJ/Mol and Enciner and Gonzalez reported the activation energy of polyethylene degradation of 137 kJ/Mol while Shao *et al.* (2001) found for polyethylene degradation an activation energy of 312 kJ/Mol.

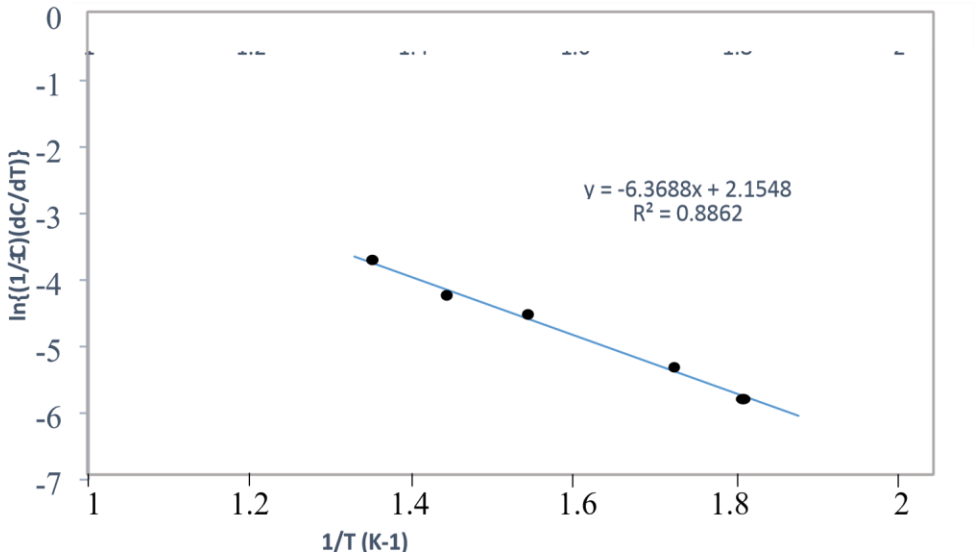

Figure 4.16: Activation Energy of mixture using Arrhenius method

The activation energy of the mixture was calculated using Arrhenius method and was found to be 52.95 kJ/Mol and a pre exponential factor of 82.26 Sec^{-1}. The obtained activation energy of the overlap organic matter of oil shale and polyethylene decomposition in the mixture which is 52.95KJ/mol is higher than that of oil shale which is 45.19 kJ/mol but less than that of polyethylene which is 153.14 kJ/mol. It is noted that the synergistic effect of the polyethylene on oil shale make the energy required low for this mixture.

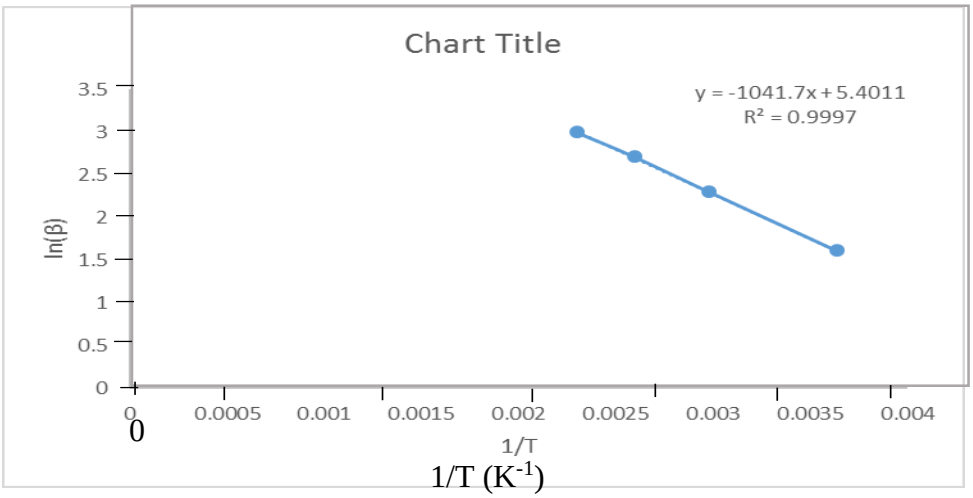

Figure 4.17: Activation Energy of Oil Shale using FWO method

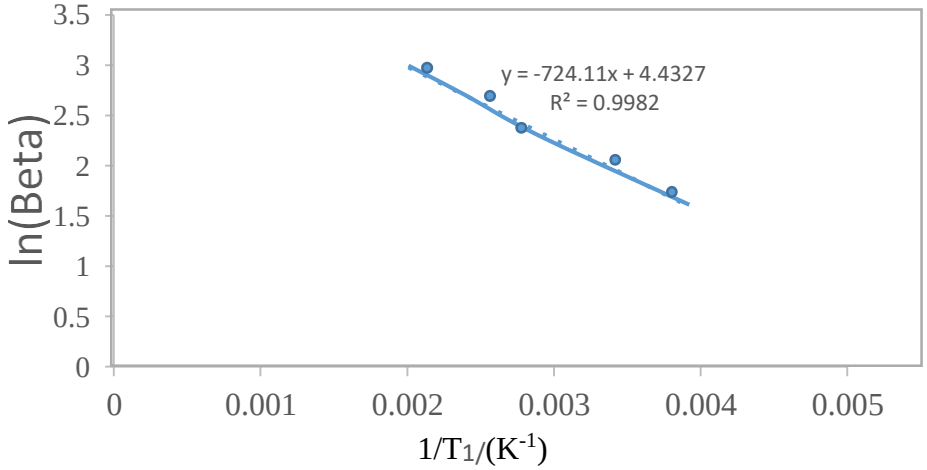

Figure 4.18: Activation Energy of Oil Shale using FWO method

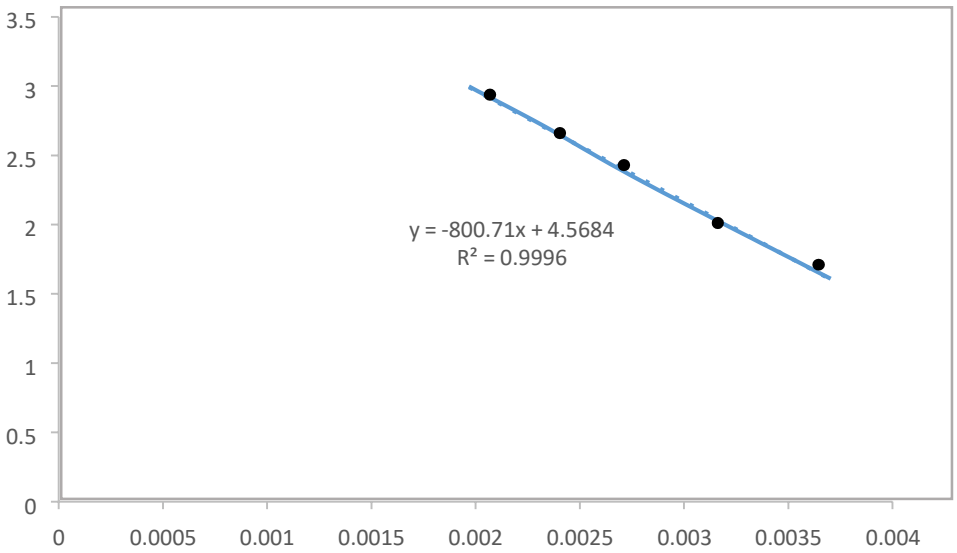

Figure 4.19: Activation Energy of Oil Shale using FWO method

Table 4.10: Activation energy with respect to conversion degree for pyrolysis and co-pyrolysis

Samples	Method	E_a (kJ/mol)	A	R^2
Oil Shale	Arrhenius	45.19	432.54	0.9568
	Flynn-Wall-Ozawa	42.00	385.91	0.9982
	Freidman	44.55	388.44	0.9902
	Coats-Redfern	46.32	413.51	0.9643
Polyethylene	Arrhenius	153.14	476.00	0.9609
	Flynn-Wall-Ozawa	156.46	441.12	0.9982
	Freidman	158.72	443.39	0.9573
	Coats-Redfern	155.41	444.04	0.95.55
Oil Shale/ Polyethylene	Arrhenius	52.95	82.26	0.9862
	Flynn-Wall-Ozawa	49.86	94.64	0.9996
	Freidman	51.04	88.97	0.9672
	Coats-Redfern	52.33	93.11	0.97381

Table: 4.10 represent the trends of the iso-conversional activation energies at each conversion degree which was calculated. Four different method was used to estimate kinetic energy of the processes. The regression coefficients of the models (R^2 value) were close to unity and they were sufficiently high enough, indicating that the models were compatible with the experimental TGA data for obtaining the activation energies of the samples. As given in the table, oil shale had an activation energy value of 45.19, 42.00, 44.55 and 46.32 kJ/mol in respect to Arrhenius, Flynn-wall-ozawa, Freidman and

CoatsRedfen method respectively while Polyethylene had an activation energy value of 153.14, 154.64, 158.72, 155.41 kJ/mol in respect to Arrhenius, Flynn-wall-ozawa, Freidman and Coats-Redfen method respectively. The activation energy for the mixture was also calculated to be 52.95, 49.86, 51.04 and 52.33 kJ/mol in respect to Arrhenius, Flynnwall-ozawa, Freidman and Coats-Redfen method respectively. Among the four models used for this work which used linear regression, the FWO method showed the best fit to the experimental TGA data for both oil shale, polyethylene and their mixture pyrolysis.

CHAPTER FIVE

5.0 CONCLUSION AND RECOMMENDATIONS

5.1 Conclusion

In this research work, pyrolysis and co-pyrolysis of oil shale and polyethylene was aimed at investigating the synergetic effect of co-pyrolysis of polyethylene and oil shale through optimization and the activation energy of the process was determined using Arrhenius and Flynn-Wall-Ozawa methods.

The results of physicochemical characterization of Ahoko oil shale and polyethylene were obtained via XRD, FTIR and TG and GCMS techniques. Design expert (Version 7.0.0, Stat Ease, Inc., USA) software was successfully applied for the prediction and optimization of oil yield in co-pyrolysis of oil shale and polyethylene at 450 to 550 ^{o}C and residence time of 90 min. The quadratic model obtained fits well to predict the response with a high determination coefficient R^2 = 0.9217. The model equation generated to predict oil yield showed that oil shale and polyethylene had relative positive impact individually on pyrolysis oil recovery from the co-pyrolysis of the mixture. Meanwhile, the co-pyrolysis at different mixture ratios showed varying quantities in the oil yield obtained.

Furthermore, the numerical optimization result revealed that maximum pyrolysis oil yield was achieved at mixture ratio 0.5 oil shale: 0.5 polyethylene. The GC–MS analysis of the oil for individual and at the optimum mixture composition hydrocarbon ranging from C_1–C_{25} shown at the peaks with the major components as alkanes, alkenes, aromatic compounds, and carboxylic acids.

Thus, it can be concluded that polyethylene acts as a hydrogen donor medium in view of its effects on oil formation during the co-pyrolysis process. The oils obtained from oil

shale, polyethylene and oil shale-polyethylene pyrolysis have the same structural properties according to elemental analysis, GC-MS and FTIR results. The kinetic parameter of the pyrolysis and co-pyrolysis of oil shale, polyethylene and mixture were calculated using Arrhenius and Flynn-Wall-Ozawa methods. From the result obtained, the activation energy (E_a) of pyrolysis of oil shale, polyethylene and mixture was calculated using Arrhenius method and found to be 45.19 kJ/mol, 153.14 kJ/mol and 52.95 kJ/mol respectively while Flynn-Wall-Ozawa method was also calculated to be 42 kJ/mol, 156 kJ/mol and 49.86 kJ/mol respectively. In comparison to the pyrolysis of individual materials, the average activation energy of co-pyrolysis declined, which indicates that polyethylene exerted synergetic effect on pyrolysis of oil shale. It was also observed that R^2 values which show the effectiveness of each of the method was giving to be 0.9997, 0.9982 and 0.9996 for Flynn-Wall-Ozawa method compared with Arrhenius method which gives 0.9568, 0.9609 and 0.9862. It can there for be concluded that Flynn-Wall-Ozawa method was more effective base on this studied. The kinetic models that were used were found to be validated with the obtained data to describe the pyrolytic and co-pyrolytic degradation mechanisms. The results obtained in this study showed that co-pyrolysis of oil shale and polyethylene could be an environmentally friendly way for the transformation of Ahoko oil shale and plastic waste into valuable products such as fuels and chemicals.

5.2 Recommendations

This research work reported on the main objectives, focusing on the co-pyrolysis of oil shale and polyethylene for oil yield and based on the findings of this study, further studies should be conducted on the physicochemicdal properties of the oil yields composition to investigate their suitability for industrial applications. In addition, possible upgrade should be considered for characteristic oil obtained.

5.3 Contribution to Knowledge

1. Ahoko oil shale has an activation energy of 42 kJ/mol and that of polyethylene is 156.46 kJ/mol while that of the mixture is 49.80KJ/mol.
2. The result of the optimization shows that the maximum yield occurred at 0.5 oil shale and 0.5 polyethylene
3. The oil yield of the mixture of oil shale and polyethylene is obtained to be 49.59%

REFERENCE

Abnisa, F., & Daud, W. M. A. W. (2015). Optimization of fuel recovery through the stepwise co-pyrolysis of palm shell and scrap tire. *Energy Conversion and Management*, *99*, 334-345.

Aboulkas, A., & El Harfi, K. (2008). Study of the Kinetics and Mechanisms of Thermal Decomposition of Moroccan Tarfaya Oil Shale and Its Kerogen. *Oil Shale*, *25*(413).

Aboulkas, A., Makayssi, T., Bilali, L., Nadifiyine, M., & Benchanaa, M. (2012). Copyrolysis of oil shale and plastics: Influence of pyrolysis parameters on the product yields. *Fuel Processing Technology*, *96*, 209-213.

Abu-Qudais, M., Jaber, J. O., & Sawalha, S. (2005). Kinetics of pyrolysis of Attarat oil shale by thermogravimetry. *Oil Shale*, *22*(1-10).

Adeoye, J. A., Akande, S. O., Adekeye, O. A., & Abikoye, V. T. (2020). Geochemistry and paleoecology of shales from the Cenomanian-Turonian Afowo formation Dahomey Basin, Nigeria: Implication for provenance and paleoenvironments. *Journal of African Earth Sciences*, *169*, 103-887.

Al-Gharabli, S. I., Azzam, M. O., & Al-Addous, M. (2015). Microwave-assisted solvent extraction of shale oil from Jordanian oil shale. *Oil shale*, *32*(3), 240.

Altun, N. E., Hwang, J. Y., & Hicyilmaz, C. (2009). Enhancement of flotation performance of oil shale cleaning by ultrasonic treatment. *International Journal of Mineral Processing*, *91*(1-2), 1-13.

Bai, F., Sun, Y., Liu, Y., Li, Q., & Guo, M. (2015). Thermal and kinetic characteristics of pyrolysis and combustion of three oil shales. *Energy Conversion and Management*, *97*, 374-381.

Bauman, J. H., & Deo, M. (2012). Simulation of a conceptualized combined pyrolysis, in situ combustion, and CO2 storage strategy for fuel production from Green River oil shale. *Energy & fuels*, *26*(3), 1731-1739.

Benbouzid, M., & Hafsi, S. (2008). Thermal and kinetic analyses of pure and oxidized bitumens. *Fuel*, *87*(8-9), 1585-1590.

Boak, J., & Kleinberg, R. (2016). Shale-and Mudstone-Hosted Oil and Gas in. *Exploration and Production of Petroleum and Natural Gas*, 373-394.

Bozkurt, P. A., Tosun, O., & Canel, M. (2017). The synergistic effect of co-pyrolysis of oil shale and low density polyethylene mixtures and characterization of pyrolysis liquid. *Journal of the Energy Institute*, *90*(3), 355-362.

Brandt, A. R. (2008). Converting oil shale to liquid fuels: Energy inputs and greenhouse gas emissions of the Shell in situ conversion process. *Environmental Science & Technology*, *42*(19), 7489-7495.

Cai, J., Wang, Y., Zhou, L., & Huang, Q. (2008). Thermogravimetric analysis and kinetics of coal/plastic blends during co-pyrolysis in nitrogen atmosphere. *Fuel Processing Technology*, *89*(1), 21-27.

Datangel, B., & Goldfarb, J. L. (2011). Heavy metals in Colorado and Chinese oil shale semicoke: disposal issues, impediments to byproduct conversion. *Energy & Fuels*, 25(8), 3522-3529.

Datta, J., & Kopczyńska, P. (2016). From polymer waste to potential main industrial products: Actual state of recycling and recovering. *Critical Reviews in Environmental Science and Technology*, *46*(10), 905-946.

Değirmenci, L., & Durusoy, T. (2005). Effect of heating rate and particle size on the pyrolysis of Göynük oil shale. *Energy Sources*, *27*(9), 787-795.

Dell, R. M., Moseley, P. T., & Rand, D. A. (2014). *Towards Sustainable Road Transport*. Academic Press.

Demirbas, A. (2016). Conversion of oil shale to liquid hydrocarbons. *Energy Sources, Part A: Recovery, Utilization, and Environmental Effects*, *38*(18), 2698-2703.

Espina, C., Straif, K., Friis, S., Kogevinas, M., Saracci, R., Vainio, H., & Schüz, J. (2015). European Code against Cancer 4th Edition: Environment, occupation and cancer. *Cancer Epidemiology*, *39*, S84-S92.

Forbes, R. J. (1970). A short history of the art of distillation: from the beginnings up to the death of Cellier Blumenthal. Brill.

Freeman, E. S., & Carroll, B. (1958). The application of thermoanalytical techniques to reaction kinetics: the thermogravimetric evaluation of the kinetics of the decomposition of calcium oxalate monohydrate. *The Journal of Physical Chemistry*, *62*(4), 394-397.

Gersten, J., Fainberg, V., Hetsroni, G., & Shindler, Y. (2000). Kinetic study of the thermal decomposition of polypropylene, oil shale, and their mixture. *Fuel*, *79*(13), 1679-1686.

Gorlov, M., Pettersson, H., Hagfeldt, A., & Kloo, L. (2007). Electrolytes for dyesensitized solar cells based on interhalogen ionic salts and liquids. *Inorganic Chemistry*, *46*(9), 3566-3575.

Herzog, A. V., Lipman, T. E., & Kammen, D. M. (2001). Renewable energy sources. *Encyclopedia of life support systems (EOLSS). Forerunner Volume-'Perspectives and Overview of Life Support Systems and Sustainable Development*, *76*.

Hoe, W. L. (2014). Probabilistic Heat Transfer in Variably Random Oil Shale Kerogen Deposit.

Juraj, T., Ľubomir, H., Jan, K., Juraj, J., & Michela, J. (2017). Evaluation of new biodegradable fluid on the basis of accelerated durability test, FTIR and ICP spectroscopy. *Research in Agricultural Engineering*, *63*(1), 1-9.

Kang, Z., Zhao, Y., Yang, D., Tian, L., & Li, X. (2020). A pilot investigation of pyrolysis from oil and gas extraction from oil shale by in-situ superheated steam injection. *Journal of Petroleum Science and Engineering*, *186*, 106-785.

Kar, T., & Hascakir, B. (2017). In-situ kerogen extraction via combustion and pyrolysis. *Journal of Petroleum Science and Engineering*, *154*, 502-512.

Kılıç, M., Pütün, A. E., Uzun, B. B., & Pütün, E. (2014). Converting of oil shale and biomass into liquid hydrocarbons via pyrolysis. *Energy Conversion and Management*, *78*, 461-467.

Koel, M., Ljovin, S., Hollis, K., & Rubin, J. (2001). Using neoteric solvents in oil shale studies. *Pure and Applied Chemistry*, *73*(1), 153-159.

Levchik, S. V., & Weil, E. D. (2004). Thermal decomposition, combustion and flame‐retardancy of epoxy resins—a review of the recent literature. *Polymer International*, *53*(12), 1901-1929.

Liu, X., Lai, J., Fan, X., Shu, H., Wang, G., Ma, X., & Luo, Y. (2020). Insights in the pore structure, fluid mobility and oiliness in oil shales of Paleogene Funing Formation in Subei Basin, China. *Marine and Petroleum Geology*, *114*, 104228.

Luik, L., Luik, H., Palu, V., Kruusement, K., & Tamvelius, H. (2009). Conversion of the Estonian fossil and renewable feedstocks in the medium of supercritical water. *Journal of Analytical and Applied Pyrolysis*, *85*(1-2), 492-496.

Ma, W., Hou, L., Luo, X., Liu, J., Tao, S., Guan, P., & Cai, Y. (2020). Generation and expulsion process of the Chang 7 oil shale in the Ordos Basin based on temperature-based semi-open pyrolysis: Implications for in-situ conversion process. *Journal of Petroleum Science and Engineering*, *190*, 107-335.

Martins, M. F., Salvador, S., Thovert, J. F., & Debenest, G. (2010). Co-current combustion of oil shale–Part 1: Characterization of the solid and gaseous products. *Fuel*, *89*(1), 144-151.

McCarthy, K., Rojas, K., Niemann, M., Palmowski, D., Peters, K., & Stankiewicz, A. (2011). Basic petroleum geochemistry for source rock evaluation. *Oilfield Review*, *23*(2), 32-43.

McKetta, J. J. (1994). Separators, Liquid-Vapor, Drum Design. *Encyclopedia of Chemical Processing and Design: Volume 49-Safety: OS1A Compliance to Separators: Vertical: Sizing with Computers*, 453.

Mochidzuki, K., Sakoda, A., & Suzuki, M. (2003). Liquid-phase thermogravimetric measurement of reaction kinetics of the conversion of biomass wastes in pressurized hot water: a kinetic study. *Advances in Environmental Research*, *7*(2), 421-428.

Mokhlisse, A., Chanâa, M. B., & Outzourhit, A. (2000). Pyrolysis of the Moroccan (Tarfaya) oil shales under microwave irradiation. *Fuel*, *79*(7), 733-742.

Popescu, C., & Segal, E. (1998). Critical considerations on the methods for evaluating kinetic parameters from nonisothermal experiments. *International Journal of Chemical Kinetics*, *30*(5), 313-327.

Quan, C., Gao, N., & Song, Q. (2016). Pyrolysis of biomass components in a TGA and a fixed-bed reactor: Thermochemical behaviors, kinetics, and product characterization. *Journal of Analytical and Applied Pyrolysis*, *121*, 84-92.

Raukas, A., & Punning, J. M. (2009). Environmental problems in the Estonian oil shale industry. *Energy & Environmental Science*, *2*(7), 723-728.

Salepcioglu, S., Gungoren, T. Ü. L. A. Y., Sert, M., Erdem, S., Saglam, M., Yuksel, M., & Ballice, L. E. V. E. N. T. (2008). Classification Of Volatile Products Evolved At Fast Co-Pyrolysis Of Göynük Oil Shale With Low Density Polyethylene. *Oil Shale*, *25*(3).

Selberg, A., Viik, M., Ehapalu, K., & Tenno, T. (2011). Content and composition of natural organic matter in water of Lake PitkJärv and mire feeding Kuke River (Estonia). *Journal of Hydrology*, *400*(1-2), 274-280.

Shao, J., Yan, R., Chen, H., Wang, B., Lee, D. H., & Liang, D. T. (2008). Pyrolysis characteristics and kinetics of sewage sludge by thermogravimetry Fourier transform infrared analysis. *Energy & Fuels*, *22*(1), 38-45.

Shuyuan, L., Zhe, Y., Jialin, Q. I. A. N., & Shaohui, G. (2001). Thermogravimetric kinetics study on some Chinese oil shales. *Oil Shale*, *18*(4), 307-314.

Speight, J. G. (2008). *The scientist or engineer as an expert witness*. CRC Press.

Taciuk, W. (2013). Does oil shale have a significant future?. *Oil Shale*, *30*(1), 1-6.

Tao, S., Wang, Y., Tang, D., Wu, D., Xu, H., & He, W. (2012). Organic petrology of Fukang Permian Lucaogou formation oil shales at the northern foot of Bogda Mountain, Junggar Basin, China. *International Journal of Coal Geology*, *99*, 2734.

Tiikma, L., Luik, H., & Pryadka, N. (2004). Co-pyrolysis of Estonian shales with lowdensity polyethylene. *Oil Shale*, *21*(1), 75-85.

Vijayakumar, A., & Sebastian, J. (2018, August). Pyrolysis process to produce fuel from different types of plastic–a review. In *IOP Conference Series: Materials Science and Engineering* 396(1), 012-062. IOP Publishing.

Vivero-Escoto, J. L., Chiang, Y. D., Wu, K. C., & Yamauchi, Y. (2012). Recent progress in mesoporous titania materials: adjusting morphology for innovative applications. *Science and Technology of Advanced Materials*, *13*(1), 013003.

Wang, S., Jiang, X., Han, X., & Tong, J. (2012). Investigation of Chinese oil shale resources comprehensive utilization performance. *Energy*, *42*(1), 224-232.

Wang, S., Jiang, X., Han, X., & Tong, J. (2014). Effect of retorting temperature on product yield and characteristics of non-condensable gases and shale oil obtained by retorting Huadian oil shales. *Fuel Processing Technology*, *121*, 915.

Wauquier, J. P. (1995). *Petroleum Refining: Crude oil, Petroleum Products,Process Flowsheets* (Vol. 1). Editions Technip.

Williams, P. T., & Ahmad, N. (2000). Investigation of oil-shale pyrolysis processing conditions using thermogravimetric analysis. *Applied Energy*, *66*(2), 113-133

Youngquist, W. (1998). Shale oil–The elusive energy. *Hubbert Center Newsletter*, *98*(4), 1-7.

Zahid, M. A., Chunmei, D., Lin, C., Gluyas, J., Jones, S., Zhang, X. & Ma, C. (2016). Sequence stratigraphy, sedimentary facies and reservoir quality of Es4s, southern slope of Dongying Depression, Bohai Bay Basin, East China. *Marine and Petroleum Geology*, *77*, 448-470.

Zhao, Y., Kang, Z., & Yang, D. (2020). Review of oil shale in-situ conversion technology. *Applied Energy*, *269*, 115-121.

APPENDICES

Appendix A: Shows the Peak list of XRD of an Oil Shale Sample

Pos. [°2Th.]	Height [cts]	FWHM Left [°2Th.]	d-spacing [Å]	Rel. Int. [%]
23.2041	50.06	0.1968	3.83336	4.86
26.6502	93.90	0.1968	3.34498	9.11
29.5466	1030.71	0.1200	3.02084	100.00
29.6192	900.71	0.0960	3.02109	87.39
31.0868	27.95	0.2880	2.87459	2.71
36.1625	84.05	0.2400	2.48191	8.15
39.6126	119.62	0.2880	2.27333	11.61
43.3629	105.45	0.2880	2.08501	10.23
47.7072	136.29	0.2880	1.90479	13.22
48.6296	126.32	0.3360	1.87079	12.26
57.5830	36.61	0.2880	1.59938	3.55
60.9482	24.97	0.7680	1.51888	2.42
64.8459	32.59	0.3840	1.43668	3.16
65.8975	19.28	0.5760	1.41628	1.87

Appendix B: Shows the Peak list of XRD of Polyethylene Sample

Pos. [°2Th.]	Height [cts]	FWHM Left [°2Th.]	d-spacing [Å]	Rel. Int. [%]
19.0900	92.37	0.2362	4.64918	7.83
20.2421	106.91	0.2362	4.38710	9.07
20.9585	799.21	0.0984	4.23873	67.77
21.1252	1179.35	0.0787	4.20566	100.00
21.3900	375.75	0.0984	4.15418	31.86
23.5083	47.42	0.1181	3.78443	4.02
25.8538	46.21	0.3936	3.44617	3.92
28.8480	146.40	0.2362	3.09495	12.41
29.1997	275.05	0.1574	3.05846	23.32
30.7610	33.32	0.3149	2.90669	2.83
31.7679	52.09	0.2362	2.81683	4.42
32.8806	16.87	0.2755	2.72401	1.43
35.7625	45.72	0.1968	2.51083	3.88
36.6127	19.70	0.3936	2.45445	1.67
42.5677	28.75	0.2362	2.12386	2.44
47.4248	37.27	0.3936	1.91706	3.16
49.0708	13.23	0.4723	1.85654	1.12
52.0362	12.61	0.3149	1.75750	1.07

57.1410	48.48	0.1574	1.61203	4.11
59.1417	4.87	0.9446	1.56218	0.41
65.6866	19.67	0.3936	1.42149	1.67

Calculation of Kinetics Energy of the Studies

Activation Energy of Oil Shale using Arrhenius method

From equation of figure 10: y = - 5.4358x + 3.7671 (A.1)

Where x = 1/T = $1/10^{-3}$ x = 10^3 x (A.2)

The slope is y = - 5.4358 X 10^3, and slope is $-\frac{E}{R}$ (A.3)

$-5.4358 \text{ X } 10^3 = -\frac{E}{R}$ (A.4)

E = R X 5.4358 X 10^3, R = 8.314 X 10^{-3} kj/Mol (A.5)

From equation 4.5

E = 8.314 X 10^3 X 5.4358 X 10^3 (A.6)

Therefore, E = 45.19 kj/mol

Note:

E =Activation Energy, In_D^AIn = Intercept (A.7)

A = DX $e_{intercept}$ (A.8)

Where D (Heating rate) = 10.0°C/min, A = pre-exponential factor,

From equation (A.8)

A = 10 x $e^{3.7671}$

A = 432. 54 sec^{-1}

Activation Energy of Polyethylene using Arrhenius method

From the Equation of figure 11: = -18.42x + 29.191 (A.9)

The slope is -18.42x 10^3, and slope is $-\frac{E}{R}$

$$-18.42\ X\ 10^3 = -\frac{E}{R} \quad \text{(A.10}$$

$$E = R\ X\ 18.42X\ 10^3 \text{ , R= 8.314 X } 10^{-3} \text{ kJ/Mol} \quad \text{(A.11)}$$

$$E = 8.314\ X\ 10^{-3}\ X\ 18.42\ X\ 10^3 = \frac{153.14KJ}{mol}$$

Therefore

E= Activation Energy $= \frac{153.14KJ}{mol}$

$$\ln\frac{A}{D} = Intercept \quad \text{(A.12)}$$

Where

$$A = Dx\ e_{intercept} \quad \text{(A.13)}$$

D (Heating rate) = 10.0°C/min, A= pre-exponential Factor

$$A = 10x\ e^{29.191} \quad \text{(A.14)}$$

$A = 4.76\ X\ 10^{2} sec^{-1}$

Activation Energy of mixture using Arrhenius method

From the Equation of figure 12, y= -6.3688x + 2.1548 (A.14)

The slope is -6.3688 x 10^3, and slope is –E/R

$$-6.3688\ X\ 10^{3} = -\frac{E}{R} \quad \text{(A.15)}$$

$E = R\ X\ 6.3688\ X\ 10^{3}$, R= 8.314 X 10^{-3} KJ/Mol

$$E = 8.314\ X\ 10^{3}\ X\ 6.3688\ X\ 10^{3} = \frac{52.95KJ}{mol} \quad \text{(A.16)}$$

E= Activation Energy $= \frac{52.95KJ}{mol}$

$$\ln\frac{A}{D} = Intercept \quad \text{(A.17)}$$

$A = Dx\ e^{intercept}$ D(Heating rate)= 10.0°C/min,

A= pre-exponential Factor

$$A = 10x\ e^{2.1548} \quad \text{(A.18)}$$

$A = 82.26 sec^{-1}$

Activation Energy of Oil Shale using FWO method

slope from graph= -1041.7 Slope from FWO = $-1.502E_R^X$

X = 0.1969

R = 0.008314
Hence; -1041.7 = -1.502E_R^X

E = (-1041.7 x 8.314)/(-1.502 x 0.1969) = 41.81KJ/mol

E = 42KJ/mol

Intercept from graph= +5.4011

Intercept from FWO = ln(AEX/Rg(X)) - 5.331 g(X) = -ln(1-X) = -ln(1-0.1969) = 0.219276039787720

Make A subject of formular 5.4011 = ln(AEX/Rg(X)) - 5.331 ln(AEX/Rg(X)) = 10.7321 AEX/Rg(X) = e(10.7321)

A = e(10.7321) x 8.314 x 0.2193 / 42 x 0.1969

A = e(10.7321) x 8.314 x 0.2193 / 42 x 0.1969 = 6.4318min-1

A = 385.908 sec-1

Activation Energy of Oil Shale using FWO method slope from graph= -724.11

Slope from FWO = -1.914EX/R

X = 0.2561

R = 0.008314

Hence; -724.11 = -1.914EX/R

E = (-724.11 x 8.314)/(-1.914 x 0.2561) = 156.46KJ/mol

E = 156.46KJ/mol

Intercept from graph= +4.4327

Intercept from FWO = ln(AEX/Rg(X)) - 4.932 g(X) = -ln(1-X) = -ln(1-0.2561) = 0.295866178

Make A subject of formular 4.4327 = ln(AEX/Rg(X)) - 4.932 ln(AEX/Rg(X)) = 9.3647

AEX/Rg(X) = e(9.3647)

A = e(9.3647) x 8.314 x 0.295866 / 156.46 x 0.2561

A = e(9.3647) x 8.314 x 0.29586 / 156.46 x 0.2561 = 7.352min-

1A = 441.12 sec-1

Activation Energy of Oil Shale using FWO method slope from graph= -800.71

Slope from FWO = -

0.261EX/RX = 0.4959

R = 0.008314

Hence; -800.71 = -0.261EX/R

E = (-800.71 x 8.314)/(-0.261 x 0.4959) = 51.43KJ/mol

E = 51.43KJ/mol

Intercept from graph= +4.5684

Intercept from FWO = ln(AEX/Rg(X)) - 7.232 g(X) = -ln(1-X) = -ln(1-0.4959) = 0.68498

Make A subject of formular 4.5684 = ln(AEX/Rg(X)) - 3.232 ln(AEX/Rg(X)) = 7.8004

AEX/Rg(X) = e(7.8004)

A = e(7.8004) x 8.314 x 0.68498 / 51.43 x 0.4959

A = e(7.8004) x 8.314 x 0.68498 / 51.43 x 0.4959 = 1.5779 min-

1A = 94.67 sec-1